STAVEBNÍ OBZOR

ČÍSLO 4/2015

Obsah čísla:

Article no. 20

THE CIVIL ENGINEERING JOURNAL 4-2015

REHABILITATION OF HISTORIC HALF-TIMBERED WALLS WITH COMPPOSITE MATERIALS BASED ON HIGH-STRENGTH

Tomáš Čejka[1], Klára Kroftová[2], Markéta Šmidtová[3] and Radek Zigler[4]

1. *CTU in Prague, Faculty of Civil Engineering, Department of Building Structures, Prague, Thákurova 7, Czech Republic; tomas.cejka@fsv.cvut.cz*
2. *CTU in Prague, Faculty of Civil Engineering, Department of Architecture, Prague, Thákurova 7, Czech Republic; klara.kroftova@fsv.cvut.cz*
3. *CTU in Prague, Faculty of Civil Engineering, Department of Building Structures, Prague, Thákurova 7, Czech Republic; smidtmar@fsv.cvut.cz*
4. *CTU in Prague, Faculty of Civil Engineering, Department of Building Structures, Prague, Thákurova 7, Czech Republic; zigler@fsv.cvut.cz*

ABSTRACT

The major requirements for present day cultural heritage conservation include the minimization of interventions in historic structures, non-invasiveness and, last but not least, reversibility of rehabilitation and strengthening interventions. Due to these requirements, composites based on high-strength fibres and epoxy resin are increasingly applied during the rehabilitation, renovation and strengthening of building structures. The article points out potential applications of these materials in the renovation, rehabilitation and strengthening of half-timbered constructions.

KEYWORDS

rehabilitation, strengthening, historic half-timbered walls, FRP fabrics

INTRODUCTION

The origins of half-timbered buildings (Fig. 1a) most likely go back to the ancient world as evidenced e.g. by Vitruvius in his Ten Books on Architecture [1]. The origins of half-timbered and timber-framed buildings which were built in the Czech lands from the 14th to the late 19th century can be traced to Germany and Scandinavian countries, but also France, Switzerland and Austria. Numerous modifications and shape patterns of wooden elements of half-timbered walls are typical and expressive architectural and decorative elements of these buildings. The buildings preserved on the territory of the Czech Republic, mainly in the northwest border regions, largely represent houses with half-timbered constructions on the upper floor and in the gable and a timbered or masonry ground floor (Fig. 1b) [1].

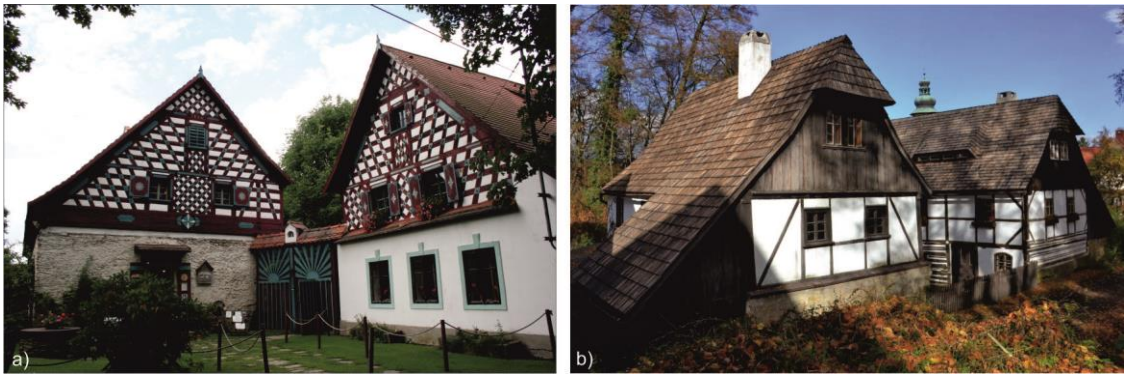

Fig. 1: Examples of half-timbered houses a) Doubrava; b) Kytlice

The term half-timbered construction denotes a wood post-frame, timber-framed or skeleton frame construction with articulated, partly rigid joints of timber elements (logs, partially squared sections, prisms) with infill panels (wattle and daub, laths, brick nogging) usually about 200 mm in thickness, inserted, in most cases, within the thickness of the wooden post-frame (half-timbered) construction. The main structural elements of half-timbered houses are the lower plate, the upper plate, posts, horizontal noggins, struts and braces. A simpler type of half-timbered framing is only composed of three horizontal beams – a plate, noggins and a ledger. In the oldest buildings, joists were always mounted on the posts to which they were directly jointed by tenons. The very construction of the half-timbered frame did not undergo any substantial changes during its historical development, except for gradual workmanship simplifications, reduction in the number of posts and diagonals and the overall robustness of the whole half-timbered construction [2,3].

DEFECTS AND FAILURES OF HALF-TIMBERED BUILDINGS

Because of its availability and ease to work with, wood, together with stone, has belonged to the most common materials used in our country in construction since the Early Middle Ages. The advantages of wood include its low weight, high compressive and tensile strength, good workability, a low coefficient of thermal expansion, good thermal insulation properties and good durability (if stored in environments with a relative humidity of 70% and protected against direct effects of water). The disadvantages of wood are heterogeneity, local defects (knots), variable mechanical properties, drying and swelling due to moisture effects (shrinkage cracks), flammability (self-ignition), low resistance to wood-destroying fungi, insects and rot and water absorption (Fig. 2), wood deformations due to compression and drying, which are greater in the direction perpendicular to grain [4].

Fig. 2: Degradation of half-timbered houses

A preliminary construction and technical survey of selected historic half-timbered constructions showed that the most common defects of timber-framed constructions were insufficient thermal insulation properties of perimeter half-timbered walls, defects and poor quality of wooden elements, workmanship defects (faulty placement of the ground plate on the plinth, poor execution of carpentry joints of wooden elements, mounting wood with high moisture, mechanical degradation of wood, excessive shrinkage and creep of wood), inappropriately applied wood treatment, absorbent material of the plinth and a generally rigid connection between internal masonry constructions (masonry walls, partitions, chimney, etc.) disabling free pushing, strain or swelling and deformations due to loading by the timbered or half-timbered construction.

The survey revealed that the main causes of failures of half-timbered buildings were inadequate foundations (settlement and deformation of foundations), deformations and strain of the timber construction due to the shrinkage (or swelling) of wooden elements, insufficient rigidity and stability, roof truss deformations, loosening of joints of wooden elements and their degradation by wood-decay agents and rotting due to elevated moisture levels, high temperatures or aggressive environments, improper use and unqualified interventions. Fig. 3 shows examples of degraded carpentry joints and wooden elements of half-timbered constructions.

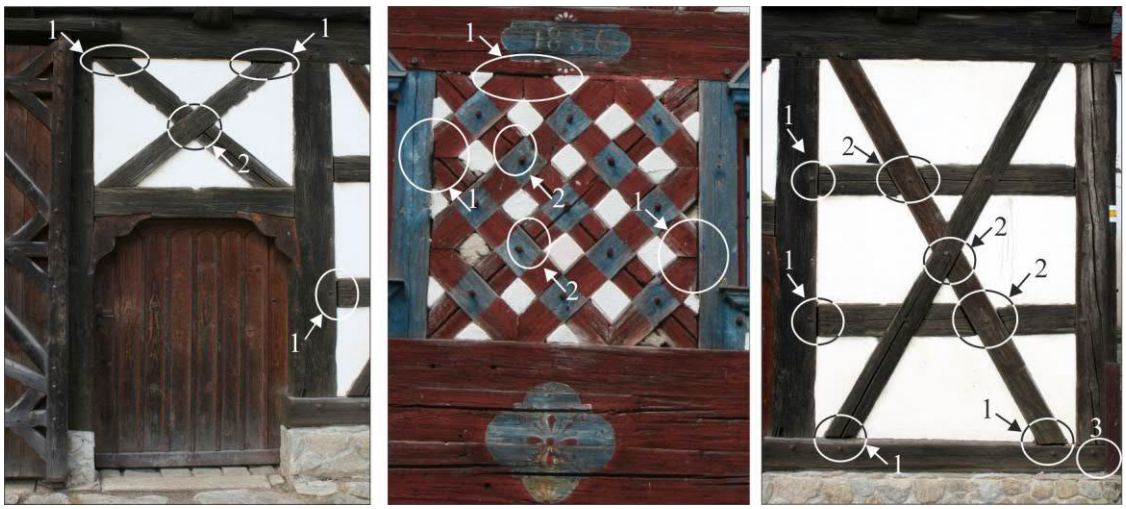

Fig. 3 Examples of failures (loosened connections) of different carpentry joints (legend 1 – tenon jointing (struts, noggins, posts), 2 – dapping (struts, noggin), 3 – halving (foundation plate)

The compression of the half-timbered frame due to wood shrinkage may reach values of up to several millimetres per meter of the wall height. This compression is prevented e.g. by the brick nogging, which, if properly wedged out, takes up part of the load transferred by the wooden frame. The loading of the joints of wooden elements due to this effect may cause the failure - loosening of connections of the half-timbered frame (Fig. 3). The joints thus created successively allow easy penetration of moisture accelerating the aging or rotting of wood.

REHABILITATION AND REINFORCEMENT OF HALF-TIMBERED BUILDINGS WITH COMPOSITE-BASED MATERIALS

While restoring and renovating historic half-timbered buildings, especially listed ones, it is necessary to preserve the original historical value of the building, prevent its further damage and the degradation of its historic construction. Permissible interventions include the restoration, conservation and stabilization of the current condition of half-timbered constructions and components – e.g. preservation of the nature and wear of a “deformed” wooden construction, including tilted floors, cantilevered ceiling parts, door framing and frames of door and window openings, only partial sealing of shrinkage joints and cracks, etc.

Loosened joints are currently wedged out during the rehabilitation or strengthened by means of suitably placed prostheses, stiffening elements, partial resin grouts, reinforcement (e.g. glass fibre connections, special steel bars), etc. Classic rehabilitation methods of timber members are used for the rehabilitation of parts of wooden or joint elements, e.g. placement of prostheses, replacement of parts of elements, etc. New and original parts of the construction are most frequently connected by carpentry joints, or joints complemented by steel bolts, pins, etc. (Fig. 4).

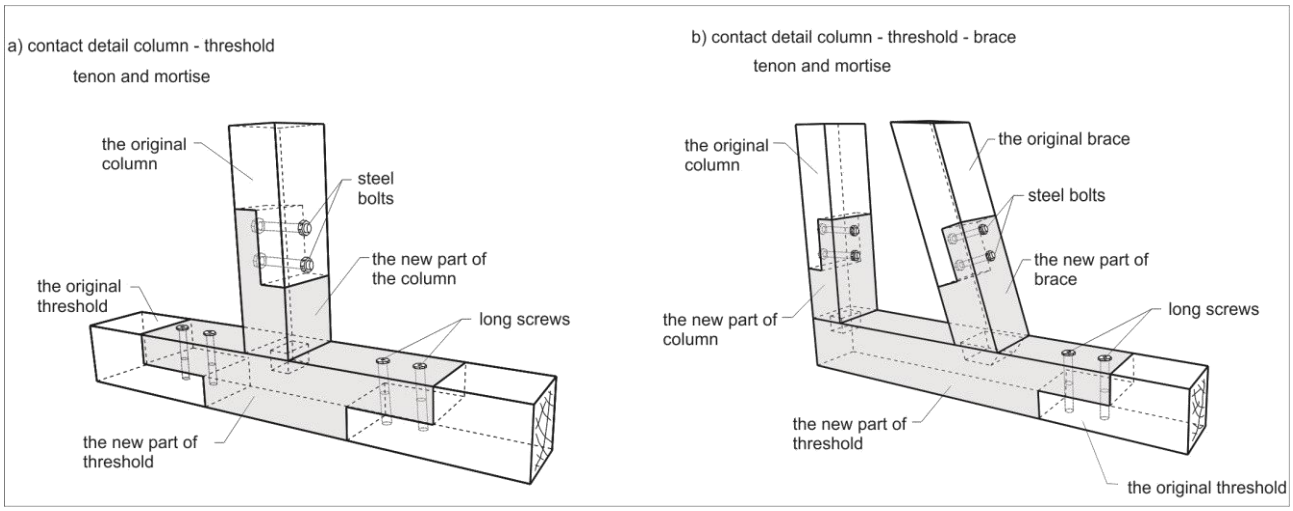

Fig. 4 Existing rehabilitation techniques of joints of elements

New possibilities in the rehabilitation of wooden elements and their joints are e.g. the surface application of diffusion-permeable fabrics based on high-strength fibres and nanofibres, or the use of lamellae based on high-strength fibre composites and epoxy resin. If the requirement for the preservation of the original appearance of the construction is raised, transparent fabrics represent a viable option. Inserting prepared lamellae or bars of composite materials in holes or grooves in wooden elements is advisable if the surface application of fabrics cannot be performed for aesthetic and heritage conservation reasons (Fig.5). While inserting strips or bars in grooves a desirable solution in this perspective may be the closure of the groove with a “splinter” of wood of the same or similar structure as the surrounding wooden part of the construction (Fig. 6). The

advantage of this solution is also enhanced fire protection of reinforcing composite strips, without the necessity of additional panelling or another modification of the construction.

If the wooden half-timbered construction acts as a spatially rigid “frame” with rigid joints (as a construction with semi-rigid joints), or as a “latticed” construction braced by diagonals and struts (spatially stable half-timbered structures without infill panels), a complex repair of the masonry infill can be performed with only partial securing of the supporting half-timbered construction during the repair. In the case of non-rigid joints and insufficient bracing of the supporting frame, the masonry infill simultaneously has a significant structurally reinforcing function. While replacing and restoring the masonry infill, this function can be substituted by using prestressing lamellae based on a composite of high strength fibres and epoxy resin, both in the vertical and horizontal direction (Fig. 5). The prestressing of the timber construction with lamellae, together with the quality assessment of the condition of joints of supporting wooden elements, the amount of bracing and the degree of rigidity, allows the removal of infill panels of the half-timbered construction and its subsequent rehabilitation.

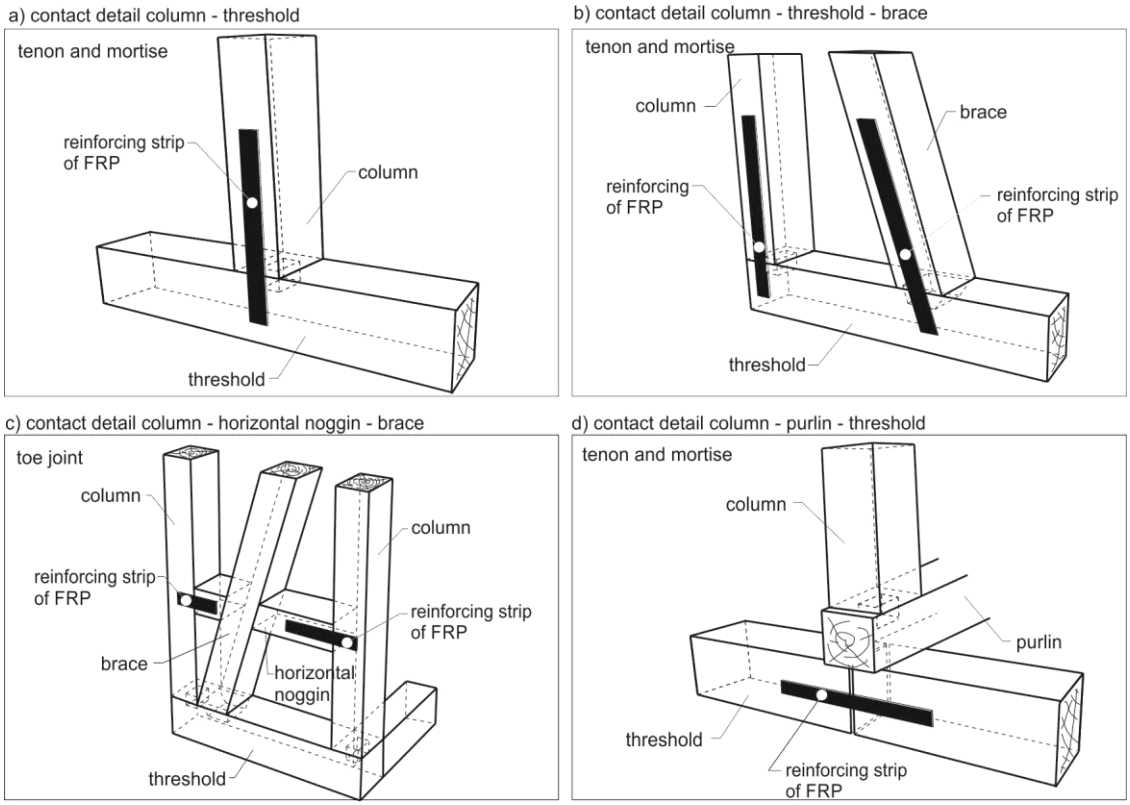

Fig. 5 Surface application of FRP fabrics for strengthening carpentry joints of half-timbered constructions

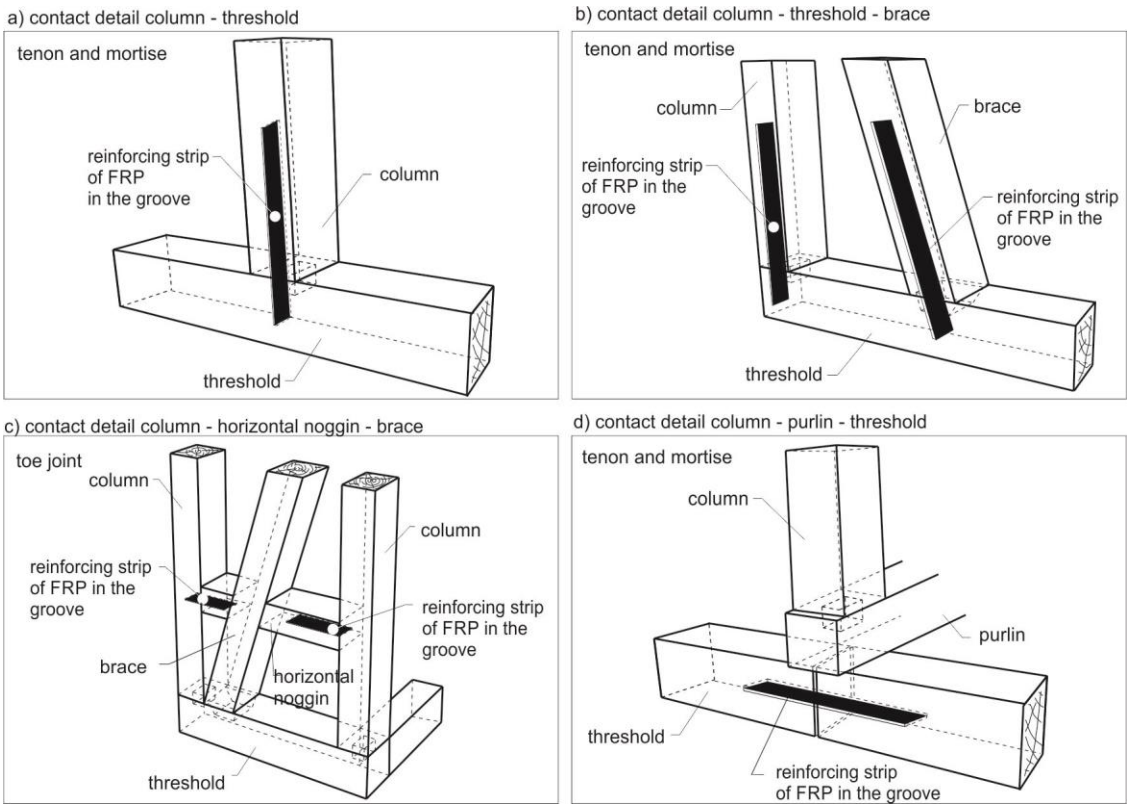

Fig. 6 Application of FRP fabrics in grooves for strengthening carpentry joints of half-timbered constructions

In less significant, unlisted buildings, major structural interventions may be designed, apart from the above specified rehabilitation measures – e.g. replacement of extensively damaged elements, strengthening of joints by means of prostheses, bolts and reinforcing sections, strengthening of elements, partial replacement of damaged parts of components, levelling deformations, stiffening the supporting structure, adding (inserting) reinforcing and supporting elements, strengthening or an extensive reconstruction of the damaged frame construction, wooden floor construction, roof truss, etc. to restore the full functionality of the construction while preserving the original nature and architecture of the building.

CONCLUSION

The application of composites based on high-strength fibres and epoxy resin for the remediation of the wooden frame of half-timbered buildings is significantly limited by the requirements for the surface quality to which they are anchored during the application of these materials. The second, no less important characteristic of these materials is high diffusion resistance limiting overall surface applications of composites on wooden structural elements of half-timbered buildings. Local rehabilitation of defects and failures of joints of wooden elements of the supporting wall construction, particularly the slippage of individual elements from the joint, is the appropriate surface application of these materials. Inserting FRP-based composite strips and epoxy resin in the grooves of wooden elements increases the fire resistance of the reinforced construction. It is advisable to use composites based on high-strength fibres and epoxy resin to improve the mechanical properties of bent elements of half-timbered constructions, mainly joists, rafters and reinforcement of roof truss joints.

ACKNOWLEDGEMENTS

The article was written with support from the NAKI DF12P01OVV037 project "Progressive Non-Invasive Methods for the Stabilisation, Conservation and Strengthening of Historic Structures and their Parts with Composite Materials Based on Fibres and Nanofibres" of the Ministry of Culture of the Czech Republic.

REFERENCES

[1] Kučová, V., Bureš, P., Principles of Folk Architecture Conservation, Nakladatelství NPÚ, Zprávy památkové péče, Praha 1999, ročník 59, ISSN 1210-5538, ISBN 80-86234-07-X (in Czech)

[2] Škabrada, J., Structures of Historic Buildings, Argo Publishing, Praha 2007, ISBN: 80-7203-548-7, EAN: 9788072035489 (in Czech)

[3] Škabrada, J., Folk Architecture: Architecture of Czech Countryside, Argo Publishing, Praha 1999, ISBN: 80-7203-082-5, EAN: 9788072030828 (in Czech)

[4] Witzany, J.et al, Failures, Degradation and Reconstruction, CTU Publishing, Praha 2010, ISBN: 978-80-01-04488-9 (in Czech)

Article no. 21

THE CIVIL ENGINEERING JOURNAL 4-2015

CONTRIBUTION TO THE POTENTIAL OF USING FRP MATERIALS IN THE REHABILITATION AND STABILIZATION OF TIMBERED BUILDINGS

Tomáš Čejka[1], Radek Zigler[2], Klára Kroftová[3] and Markéta Šmidtová[4]

1. *CTU in Prague, Faculty of Civil Engineering, Department of Building Structures, Prague, Thákurova 7, Czech Republic; tomas.cejka@fsv.cvut.cz*
2. *CTU in Prague, Faculty of Civil Engineering, Department of Building Structures, Prague, Thákurova 7, Czech Republic; zigler@fsv.cvut.cz*
3. *CTU in Prague, Faculty of Civil Engineering, Department of Architecture, Prague, Thákurova 7, Czech Republic; klara.kroftova@fsv.cvut.cz*
4. *CTU in Prague, Faculty of Civil Engineering, Department of Building Structures, Prague, Thákurova 7, Czech Republic; smidtmar@fsv.cvut.cz*

ABSTRACT

Wooden log, timbered perimeter and interior walls ranked among the most common building constructions used from the Early Middle Ages. In most cases, the local natural resources, i.e. wood, clay, straw and stone, were used for building houses with wooden framing. This article outlines typical defects and failures of timbered houses, “classic” techniques for the rehabilitation of these defects and failures indicating the potential of using composite materials based on high-strength fibres and epoxy resin in the rehabilitation and strengthening of timbered buildings.

KEYWORDS

rehabilitation, strengthening, timbered buildings, FRP fabrics

INTRODUCTION

The timbered constructions (Fig. 1), whose origins may be traced to mainly Central and Eastern Europe, were a widespread construction technology for residential and farm buildings used in our country from the Early Middle Ages. After the 12th century, timbered houses represented the predominant type of residential development on our territory, and their use in rural areas prevailed until the late 18th and the early 19th century, in northern and western Bohemia even until the late 19th century. The decline of building timbered constructions was primarily due to the prohibition of wooden constructions because of the risk and spread of fires in 1816. According to Schedel’s World Chronicle from the end of the 15th century, timbered framing was also found in urban buildings. There are timbered houses with a timbered wall construction on the ground floor and their upper floor construction is supported on the so-called pedestal formed by protruding columns and beams (ground plates) and constructions with a single living space resting on a masonry, mostly stonework, construction.

Fig. 1: Examples of timbered houses a) Příbram; b) Přerov nad Labem

Timbered walls are usually made of horizontally mutually superposed solid logs or beams, most often joined in corners by the dovetail joint, or a dovetail joint with opposite inclined sides without overlaps to prevent the bond loosening and beam slippage; there may also be gaps between slabbed sections. From the late 18th century, the above bond was replaced by more demanding, so-called interlocks, with perpendicularly cut horizontal and vertical surfaces – mortises with perpendicular walls. Figs. 2a, 2b and 2c show examples of carpentry corner joints of timbered buildings. The gaps between horizontal wall elements were sealed with moss and subsequently puddled with clay, cob, reinforced with straw, animal hair, etc.

Fig. 2: Examples of carpentry corner joints of timbered houses

The ceiling of the timbered construction was made of timber girder floors or logs, either planar or cranked up to reach the roof truss at the strutting beam and rafter level; the so-called log or timbered wooden vault with joints between the logs of the floor construction was puddled with cob.

Typical features of historic timbered buildings are gable roofs or gable roofs with small hipped ends, greatly extending beyond the perimeter structure and protecting it against the weather.

DEFECTS AND FAILURES OF TIMBERED BUILDINGS

The most frequent causes of failures of log and timbered buildings include particularly volume changes of the wooden construction of timbered walls. These changes are caused by

shrinkage, the attacks of wood-destroying fungi and insects or by rot, and are often accompanied by strong non-uniform vertical deformations of the timbered wall and a loss in the mechanical properties of wood which may reach values affecting stability. For this reason, timbered walls were reinforced and their stability was secured by wooden pegs (vertical pins), square dowels (short chips) inserted in the grooves cut across the logs mainly close to holes and often protruding to the timbered wall face, or they were interconnected with lath inserts, hammered iron blades, etc. (Škabrada, 2007).

The most common defects of half-timbered and timbered constructions include insufficient thermal insulation properties of perimeter timbered walls, defects and poor quality of wooden elements, workmanship defects, faulty placement of ground plates on the plinth, poor execution of joints of wooden elements, mounting wood with high moisture levels, mechanical degradation of wood, mounting wooden elements with high moisture levels, excessive shrinkage and creep, inappropriately applied wood treatment, absorbent material of the plinth and a generally rigid connection between interior masonry constructions (Fig. 3).

Fig. 3: Degradation of timbered houses

The deformation of timber (coniferous wood was mostly used) due to the effect of compression and drying is more significant in the direction perpendicular to grain. For this reason, particularly log and timbered walls suffer from considerable creep, which, depending on the size (cross section) of beams (or logs) can reach up to several tens of millimetres (long-term pushing – “creep” – a multiple increase in initial deformations). This leads to the deformation of the wooden construction of the building, the deformation and tilting of the ceiling joist or slab construction, sloping of window and door openings and damage to interior masonry “auxiliary” constructions.

RESTORATION OF TIMBERED AND HALF-TIMBERED BUILDINGS

While restoring historic timbered and half-timbered buildings, especially listed ones, it is necessary to preserve the original historical value of the building, prevent its further damage and the degradation of the historic construction and, above all, extend the life of the listed structure. Based on a detailed historical, construction and technical survey (or other surveys), the restoration work sequence may be designed in an expert way to avoid any losses in the building’s value.

In the construction and technical perspective, the rehabilitation of damaged structural members and joints may be carried out as follows. Loosened connections must be wedged out or strengthened with suitably placed prostheses, stiffening elements, partial resin grouts, reinforcement (e.g. glass fibre connections, special steel bars), etc. (Fig. 4).

Wooden elements and their connections may also be rehabilitated using diffusion-permeable and transparent fabrics of high strength fibres and nanofibres. In less significant, unlisted buildings, the major structural interventions may be designed, apart from the above specified rehabilitation measures, to reach a reasonable conformity to the current requirements for the indoor environment quality without compromising the original architectural character and the historical value of the building.

Fig. 4: Rehabilitation of elements and joints of timbered wall using the classic method – replacement, sealing

The possibility of using composite materials based on high-strength fibres and epoxy resin in the renovation of timbered buildings is primarily affected by the loading pattern of the joints used for the interconnection of individual beams into walls, both in corners or along the elements' height.

In the case of vertical structures, the use of prestressing or non-prestressed composite strips based on high-strength fibres and epoxy resin is preferred to capture the horizontal forces exerted by the roof truss to avoid the tilting of timbered walls - opening up of the building - and the slippage of the upper beams of the wall. It is advisable to place these strips on the surface of joists (Fig. 5) and anchor them to the outer wall surface. The composite strips placed in this way increase the rigidity of the building and may partly replace transverse (interior) timbered walls securing the spatial stability and rigidity of the construction.

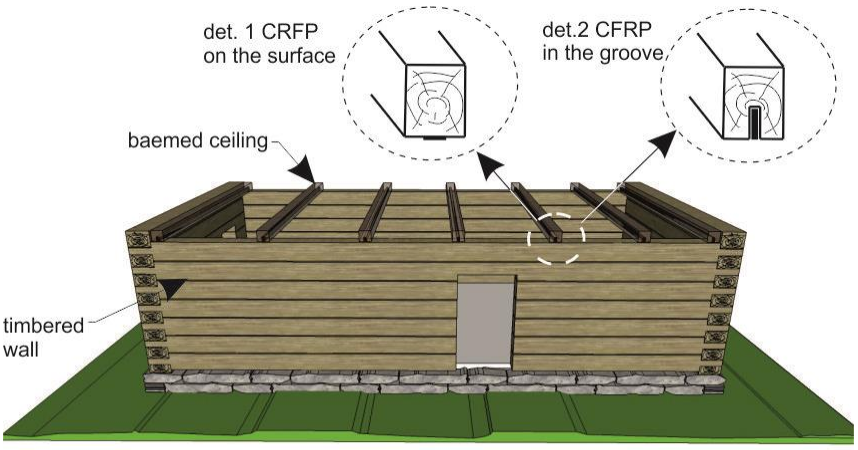

Fig. 5: Securing the spatial rigidity of a timbered construction in the case of degraded tie beams – reinforcing FRP strips or lamellae are led along the surface or in the groove of joists and anchored to the outside

surface of timbered walls

In the case of a multi-storey timbered building, like in a masonry building, adding a “reinforcing collar beam” at the floor construction level over the 1st overground storey using prestressing lamellae may be an effective solution (Fig.6).

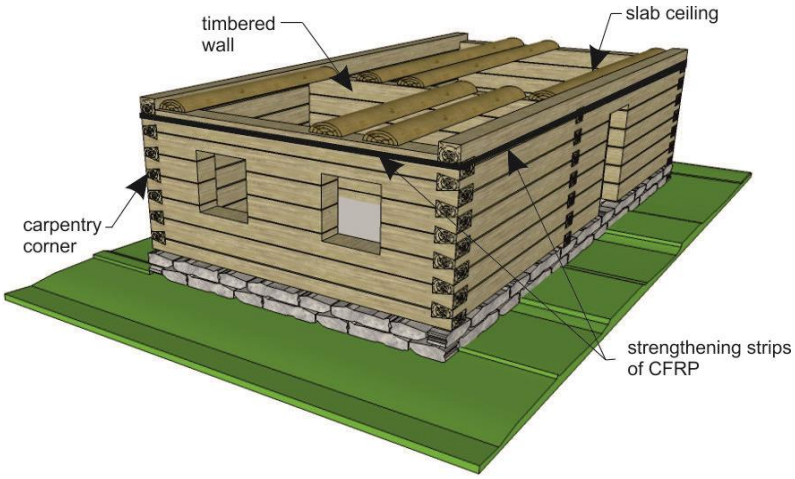

Fig. 6: Securing the spatial rigidity of a timbered construction by a reinforcing collar beam at the floor construction level

Vertical bracing or prestressing of joints of horizontal members (corners of the building) with composite strips based on high-strength fibres and epoxy resins limits the potential slippage of individual members from the joint in the case of degraded dovetail joint surfaces. It is advisable to place vertical stiffening strips or lamellae in the vertical groove to ensure the functionality of the joint reinforcement increasing, at the same time, the fire resistance of the remediation measure. This remediation method requires the adjustment of the anchoring surfaces of wooden elements so that they are cohesive, planar, without increased moisture contents (Fig. 7).

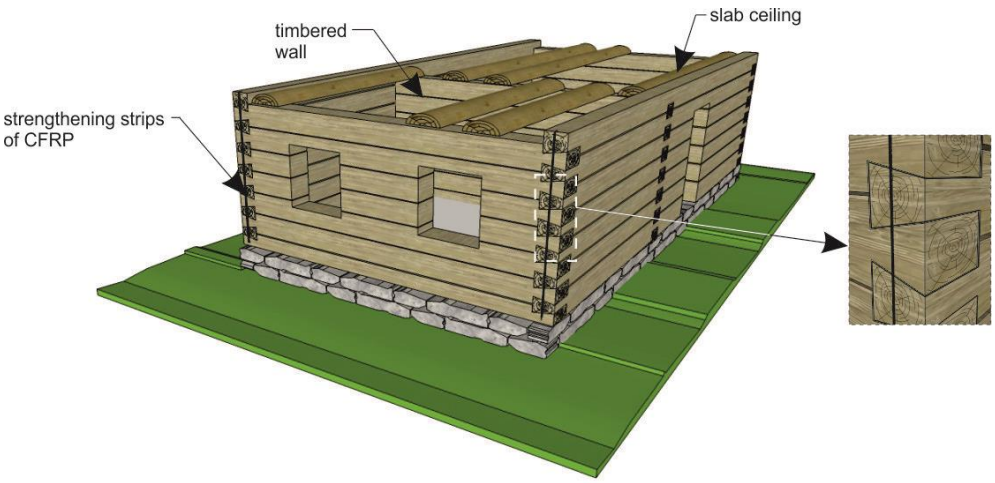

Fig. 7: Vertical stiffening of beam joints – limitation of the slippage of wall elements from joints, enhanced resistance of the timbered construction to seismic effects

The disadvantage of using composite materials based on high-strength fibres and epoxy resins is their high diffusion resistance, which, in the case of larger surface applications, may be

the cause of an increase in the moisture content of a wooden structural member and associated degradation and biodegradation processes.

Anchoring elements allowing the elimination of volume changes of wood should be used in the case of using composite materials based on high-strength fibres and epoxy resin, mainly lamellae, in order to increase the spatial rigidity and secure the stability of a timbered construction.

CONCLUSION

The application of composite materials based on high-strength fibres and epoxy resin in timbered constructions is advisable, if the parts of the construction capturing horizontal forces from the roof truss are damaged or loosened, to prevent the tilting or falling apart of the supporting structure (e.g. walls).

Due to the properties of wood (especially in relation to volume changes caused by moisture or degradation processes) and the type of timbered structure and joints of wooden wall elements, the beneficial application of composite materials based on high-strength fibres and epoxy resin is limited to mainly the stabilization and reinforcement of the floor construction members and roof truss elements and joints.

ACKNOWLEDGEMENTS

The article was written with support from the NAKI DF12P01OVV037 project "Progressive Non-Invasive Methods for the Stabilisation, Conservation and Strengthening of Historic Structures and their Parts with Composite Materials Based on Fibres and Nanofibres" of the Ministry of Culture of the Czech Republic.

REFERENCES

[1] Kučová, V., Bureš, P., Principles of Folk Architecture Conservation, Nakladatelství NPÚ, Zprávy památkové péče, Praha 1999, ročník 59, ISSN 1210-5538, ISBN 80-86234-07-X (in Czech)

[2] Pešta, J., Rekonstrukce roubených staveb/Reconstruction of Timbered Buildings, Grada Publishing, Praha 2013, ISBN 978-80-247-3239-8 , (in Czech).

[3] Škabrada, J., Structures of Historic Buildings, Argo Publishing, Praha 2007, ISBN: 80-7203-548-7, EAN: 9788072035489 (in Czech)

[4] Škabrada, J., Folk Architecture: Architecture of Czech Countryside, Argo Publishing, Praha 1999, ISBN: 80-7203-082-5, EAN: 9788072030828 (in Czech)

[5] Witzany, J.a kolektiv, Failures, Degradation and Reconstruction, CTU Publishing, Praha 2010, ISBN: 978-80-01-04488-9 (in Czech)

Article no. 22

THE CIVIL ENGINEERING JOURNAL 4-2015

FIRE PROTECTION OF TIMBER STRUCTURES STRENGTHENED WITH FRP MATERIALS

Radek Zigler[1] and Marek Pokorný[2]

1. Czech Technical University, Faculty of Civil Engineering, Department of Building Structures, Thárukova 7, 166 29, Prague 6,, Czech Republic; zigler@fsv.cvut.cz
2. University Centre for Energy Efficient Buildings of Czech Technical University in Prague, FireLAB, Třinecká 1024, 273 43 Buštěhrad, Czech Republic; marek.pokorny@cvut.cz

ABSTRACT

Modern, progressive methods of structures' strengthening based on the use of composite materials composed of high strength fibers (carbon, glass, aramid or basalt) and matrices based on epoxy resins brings, among many indisputable advantages (low weight, high effectiveness, easy application etc.) also some disadvantages. One of the major disadvantages is a low fire resistance of these materials due to the low glass transition temperature T_g of the resin used. Based on an extensive research of strengthening of historic structures with FRP materials [1], the article outlines possible approaches to this problem, especially while strengthening timber load-bearing structures of historic buildings.

KEYWORDS

timber, strengthening, joint stabilization, FRP, fire protection

INTRODUCTION

Timber structures are significant part of load bearing structures of historic buildings (buildings built around the 1st half of the 20th century), such as roof trusses, corduroy (log) or beamed ceilings, internal skeletons, etc. While reconstructing these buildings, we often face the necessity of strengthening individual wooden elements or their connections. Traditionally, wood and steel in the form of various straps or prostheses or in the form of additional fasteners is used. In the last decade, new progressive FRP (Fiber Reinforced Polymers) based methods are being used. These methods use composite materials composed of a matrix (usually an epoxy resin) and reinforcing fibers (mostly carbon and glass, less often aramide, basalt or natural fibers). Depending on the type of fibers used the resulting strength of composite ranges from 500 to 2000 MPa. Similarly, the elastic modulus reaches values up to 250 GPa. The advantages of FRP materials lie in their high tensile strength, low weight, and their ability to conform to varying shapes. The versatility and ease of installation make FRP retrofit solutions extremely effective. One of the limiting factors is the low fire resistance of FRP materials and therefore the need for additional fire protection of strengthened or stabilized timber structures.

STRENGTHENING OF TIMBER STRUCTURES WITH FRP MATERIALS

The reinforcement of structural timber elements is designed to supplement the ductile behaviour of such elements. This can be improved by forcing the ratio between ultimate tensile strength and ultimate compressive strength with higher ultimate strength. This result can be achieved by improving the behaviour of the tension zone so as to permit a plastic behaviour in the compression zone. This amounts to taking full advantage of the material properties, resulting in higher ductility at collapse.

For strengthening of timber elements stressed mainly by bending or shear, FRP materials (in the form of lamellas, rods, or fabrics) placed on the surface of strengthened element (Externally Bonded Reinforcement - EBR) or in the grooves near the surface (Near Surface Mounted - NSM) are used. FRP materials can also be used to stabilize or strengthen joints of the wooden elements. Fig. 1 shows some examples of possible strengthening interventions for timber load bearing elements and Fig. 2 shows examples of the possible joint stabilization or strengthening. In all cases, it is vital that the adhesive used for the bonding of wood in structural applications should be characterised by high shear strength and good compatibility with different kinds of wood types [2].

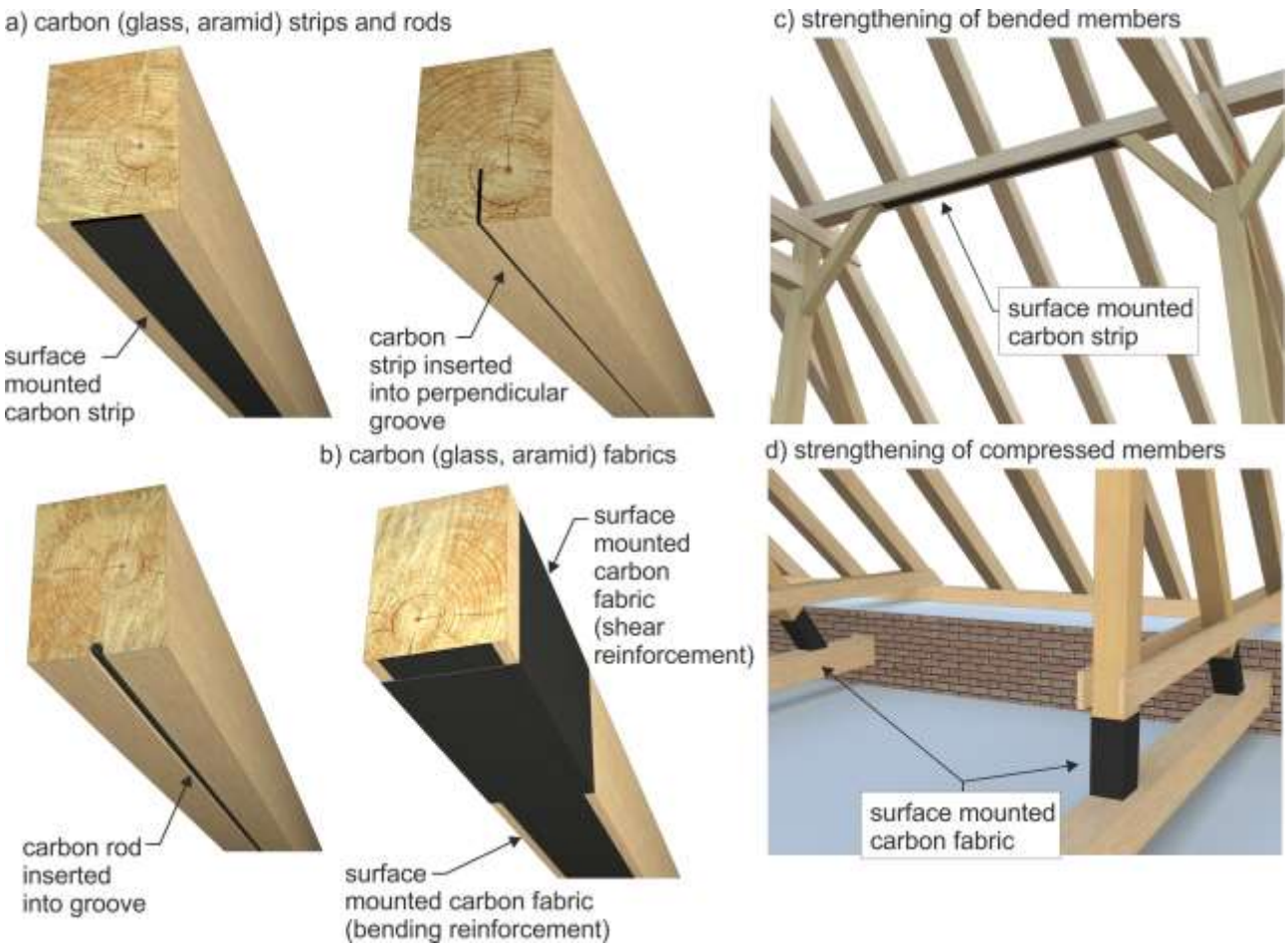

Fig. 1 Examples of strengthening of timber structures using externally bonded FRP materials (EBR)

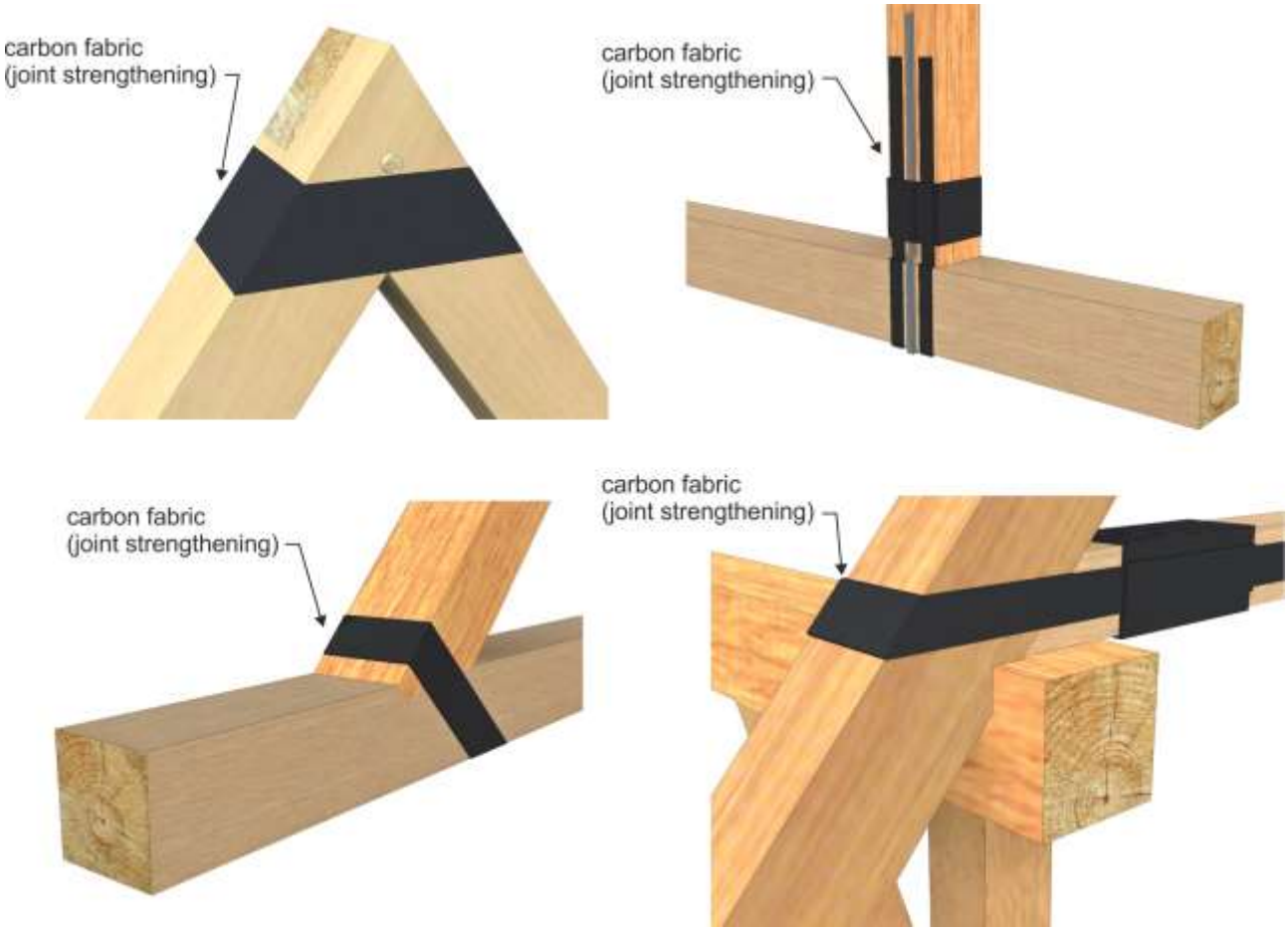

Fig. 2 Examples of possible joint stabilization and strengthening using externally bonded FRP materials (EBR)

WOOD BEHAVIOUR IN FIRE CONDITIONS

The behavior of wood in the fire conditions is sufficiently theoretically and experimentally described. The fire resistance of unprotected wood element is usually determined by standard procedures pursuant to Eurocodes (EN 1995-1-2) [3], which provide two different methods for determining the fire resistance - method of reduced timber properties in fire conditions and method of reduced (weakened) cross-section as a result of surface charring of the wood element. A tabular (rather conservative) approach is often used in practice for determining a structure's fire resistance [4] based on Eurocodes or tabular approach based on the national standards (eg. ČSN 73 0821 ed. 2 [5], ČSN 73 0834 [6]). In case of fire protected timber structures, in particular using external encasing, the limit temperature of layers can be considered 120 °C while the glowing temperature, according to the wood type used ranges from 200 to 300 °C (ČSN 73 0810 [7]).

The temperature of the non-charred part of the section during the fire resistance period does not usually exceeds 110-120 °C. Therefore the limiting strength of the wood during fire can be considered the value of strength of wood at 120 °C. The decrease in strength depends directly on the temperature and indirectly on moisture content in wood. The burning rate increases with the content of resin, fats, etc., and decreases with increasing moisture content and density of wood. The burning and ignitability of wood also depends on the surface quality and surface finish, its

dimensions and porosity. Experimental research of wooden elements (spruce beams) exposed to a standard fire demonstrated an average speed of burning off the surface layers in the direction to the core cross-section from the side of 0.65 mm/min and from below 0.95 mm/min. Joints of individual wood members are other very sensitive part of timber structures, especially for roofs trussed and load bearing skeletons. Original wooden fasteners (e.g., pins, wedges, liners etc.) were later usually replaced by steel fasteners (e.g. bolts, screws, dowels etc.). For these fasteners their thermal conductivity must be respected as they will warm faster due to the increasing thermal conductivity. The heat is also transmitted to the connected wood members [8].

FRP BEHAVIOUR IN FIRE CONDITIONS

One of the characteristics of FRPs is their low glass transition temperature (T_g). T_g is the midpoint of the range of temperatures over which the FRP polymer matrix undergoes a change from hard and brittle to viscous and rubbery. Polymer matrices that cure at room temperature and are often used for structural strengthening have glass transition temperatures T_g ranging from 60°C to 130°C. At temperatures above 400 °C, FRPs are susceptible to combustion of polymer matrix and can even evaporate [9]. Without protection from heat, a polymer matrix may also ignite, emit smoke, and support spreading of flame. When exposed to fire, FRP materials may suffer charring, melting, delamination, cracking and deformation. Figure 3 shows that for some types of matrices, debonding can be well advanced at 200°C. It also shows that the fibers themselves lose strength with rising temperatures, with carbon fiber losing the least.

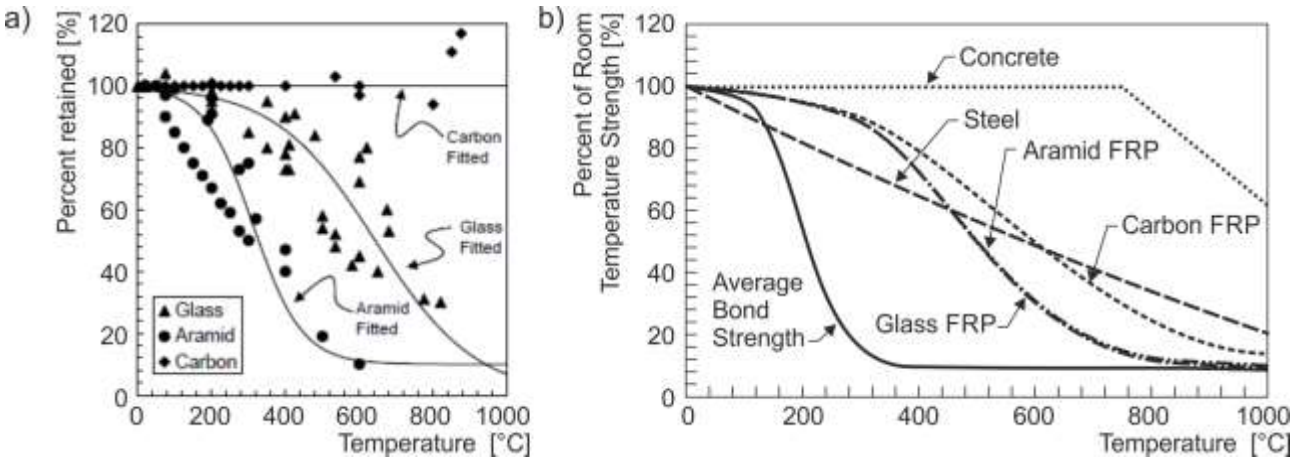

Fig. 3. Approximate variation in tensile strength and bond strength with temperature increase; a) Bare fiber strength [10]; b) FRP, concrete and reinforcing steel [11]

Therefore, it is apparent that a fire protection for structural elements reinforced with FRP materials is essential and that even small temperature increase in FRP-wood contact can have a profound effect on the resulting load bearing capacity and static function of the strengthened timber member or joint.

Experimental research conducted on masonry [12] and concrete structures [11], [13], [14], [15] demonstrated the sufficient usability of externally bonded FRP reinforcement during fire, if the structure is adequately fire protected.

FIRE PROTECTION OF TIMBER STRUCTURES STRENGTHENED WITH FRP MATERIALS (EBR, NSM)

There are some methods traditionally used for fire protection of timber structures that are also suitable for fire protection of structures strengthened and stabilized with FRP materials such as encasing, mineral fiber coverings and fire resistant plasters. The encasing or fire protection boards are usually based on gypsum, vermiculite, cement, or on lime and cement combination. Mineral fiber coverings are normally basalt based. Fire resistant plasters may be gypsum-perlite, gypsum-vermiculite based, gypsum, gypsum-lime, lime, lime-cement or cement based. In all cases it is necessary to take into consideration the possibility of the element encasing or plastering, both in terms of heritage protection requirements (valuable ornate features of beamed ceilings, roof trusses etc.), and the possible wood degradation due to the encasing (all timber structures that are enclosed in non-porous encasing materials must treated against possible biodegradation).

Methods based on fire retardant coatings are not suitable, especially the use of foam-forming (intumescent) materials that activate (start to foam) only at temperatures higher than the critical - glass transition - temperatures T_g of the epoxy resin.

On the other hand the use of fire protective cladding based on wood elements with sufficient thickness can be applied to protect the FRP strengthened elements. The use of wood cladding appears to be the best option in particular for timber elements reinforced with FRP materials inserted into grooves (NSM). In this case the wooden cladding fulfills both the fire protective and aesthetic functions (Fig. 4).

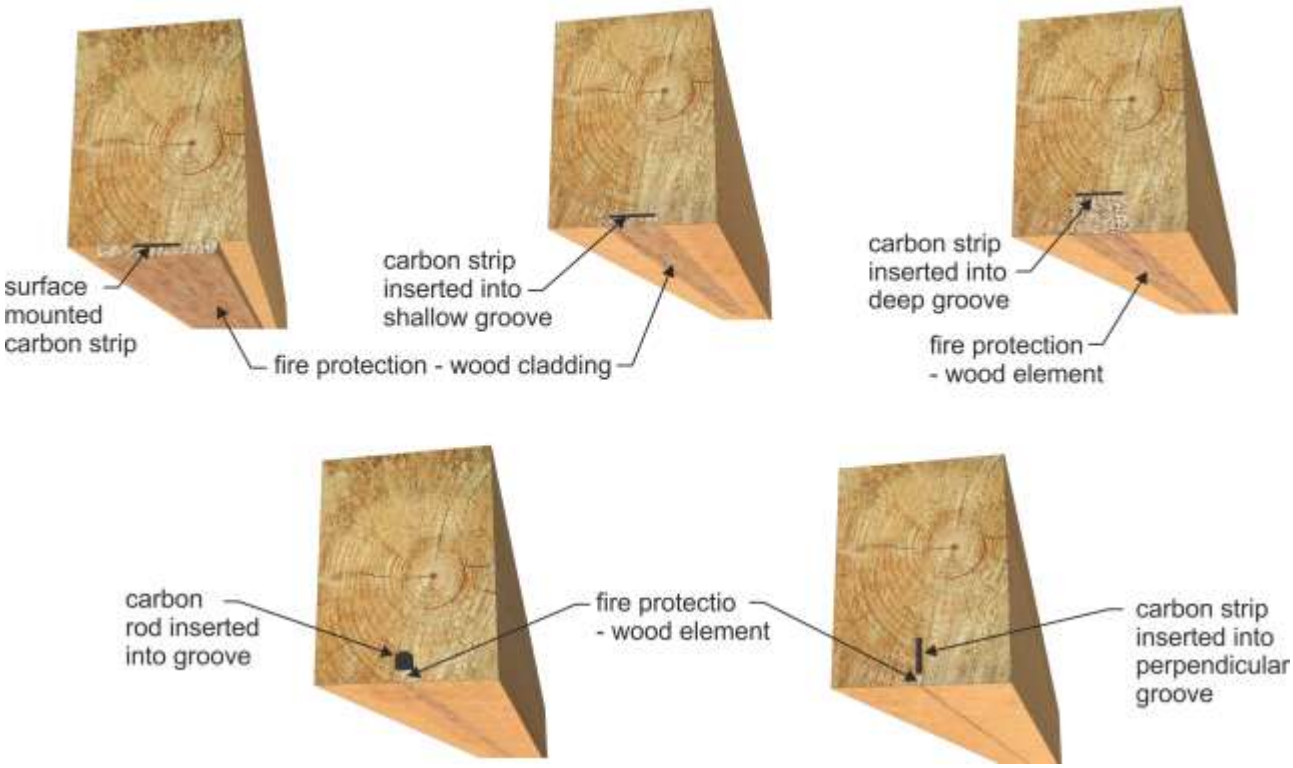

Fig. 4 Fire protection of strengthening FRP elements

To determine the required thickness of the wood cladding needed, a simple parametric study with the following initial and boundary conditions was performed:

- one-dimensional calculation of heat transmission with the use of software Argos (DBI, version 5.8.92.414 [16])
- fire exposure with the nominal standard temperature curve according to ISO 834 [17]
- starting temperature 20 °C, heat transfer coefficient 25 W/(m^2.K) on the side exposed to the fire and 7.7 W/(m^2.K) on the opposite side, surface and fire emissivity 0.9
- two different thicknesses of softwood spruce cladding – 25 mm and 40 mm
- gradual charring expressed by change in density, thermal conductivity and specific heat capacity for the protective cladding was considered (values according to ČSN EN 1995-1-2, Tab. B.2 [3])
- critical - glass transition - temperature T_g of the FRP system was considered 100 °C (depending on the polymer matrix used, temperatures ranging between 60 and 130 °C are mentioned in literature [12]

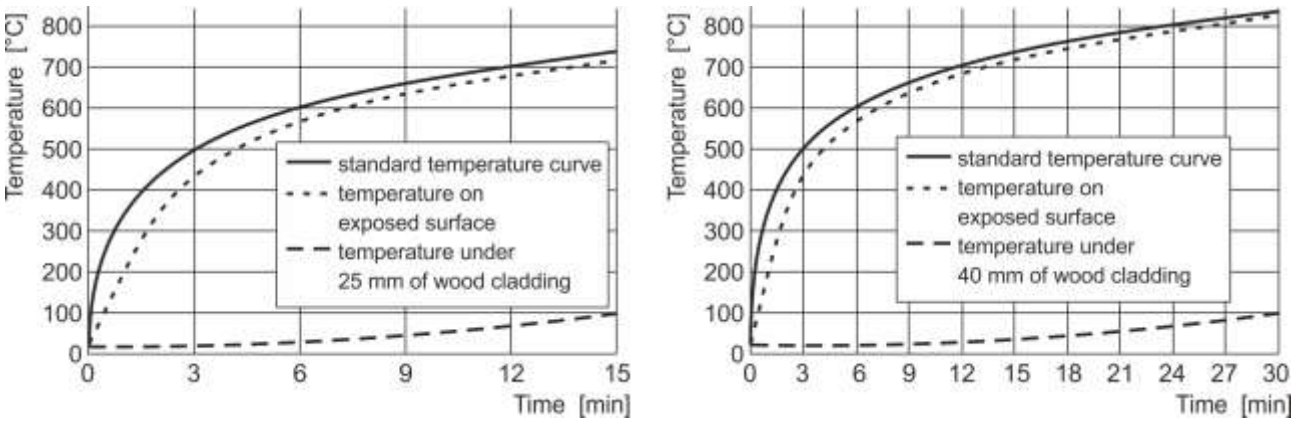

Fig. 5 Temperatures at the FRP reinforcement in case of fire protection system using wood cladding 25 mm (left) and 40 mm (right) thick

The parametric study results show that the wooden cladding with thickness of 25 mm under the conditions of standard fire can provide a critical temperature of the FRP bellow 100 °C for a maximum period of about 15 minutes (Fig. 5, left). If the cladding thickness is increased to 40 mm, fire protection for about 30 minutes (Fig. 5, right) can be achieved.

CONLUSION

Fire protection of a FRP strengthening system providing the required fire resistance of the strengthened structural member must be dealt with especially when the structural element is in the fire zone of a usable storey (e.g. visible elements of the roof truss in the attic). However, if the structural element is situated in a non-usable storey, eg. an unused attic or roof-cavity space (usually above the fire ceiling) the fire risk is not calculated, fire resistance of the structure is not required and therefore the strengthened member, including the strengthening FRP system can be entirely without fire protection.

If a fire protection is needed, simple encasing with wood elements (cladding) of sufficient thickness can provide the necessary fire resistance of a strengthened or stabilized timber member. Especially, the near surface mounted FRP systems are highly suitable for this kind of fire protection as it also provides the necessary aesthetic requirements.

If the encasing is not possible (due to various reasons) or the required fire resistance is higher than 30 minutes (which would require thicker encasing elements and would be problematic from the point of technology and static efficiency), epoxy matrices with higher glass transition temperatures T_g [9], or other types of bonding materials may be used (such as FRG or FRCM systems).

ACKNOWLEDGEMENTS

The paper was written with support from the Czech Ministry of Culture research project NAKI DF12P01OVV037 “Progressive non-invasive methods of the stabilization, conservation and strengthening of historical structures and their parts with fibre- and nanofibre-based composite materials”.

REFERENCES

[1] Czech Ministry of Culture research project NAKI DF12P01OVV037 " Progressive non-invasive methods of the stabilization, conservation and strengthening of historical structures and their parts with fibre- and nanofibre-based composite materials", 2012-2015, lead researcher prof. Ing. Jiří Witzany, DrSc.

[2] Bernardini C, Credali L. and Pistone G, 2007. Strengthening Of Wooden Beams with FRP Materials, edited by S. T. Smith (Asia-Pacific Conference on FRP in Structures - APFIS 2007), 297-304

[3] ČSN EN 1995-1-2 Eurocode 5: Design of timber structures - Part 1-2: General - Structural fire design, UNMZ 2006

[4] Zoufal R. et al., 2009. Hodnoty požární odolnosti stavebních konstrukcí podle Eurokódů. (PAVUS a.s., Praha) ISBN 978-80-904481-0-0.

[5] ČSN 73 0821 ed. 2 Fire protection of buildings - Fire resistance of engineering structures, UNMZ 2007

[6] ČSN 73 0834 Fire protection of buildings - Changes of buildings, UNMZ 2011, 2013

[7] ČSN 73 0810 Fire protection of buildings - General requirements, UNMZ 2009

[8] Kupilik V., 2006. Stavební konstrukce z požárního hlediska, (Grada Publishing, Praha) ISBN 80-247-1329-2

[9] Gefu J., Guoqiang L., Walid A., 2013. A new fire resistant FRP for externally bonded concrete repair, Construction and Building Materials, vol. 42: 87-96, DOI: 10.1016/j.conbuildmat.2013.01.008

[10] Green M.F., Benichou N, Kodur V.K.R., Bisby L.A., 2008. Design Guidelines for Fire Resistance of FRP-Strengthened Concrete Structures (Eighth International Conference on FRP in Reinforced Concrete Structures FRPRCS-8), 1-10

[11] Williams, B., Bisby, L., Kodur, V., Green, M., Chowdhury, E., 2006. Fire insulation schemes for FRP-strengthened concrete slabs, Composites Part A: Applied Science and Manufacturing, 37: 1151-1160. DOI: 10.1016/j.compositesa.2005.05.028

[12] Zigler, R., Pokorný, M., 2015. Požární zkouška chování zděných cihelných pilířů zesílených pásky na bázi vysokopevnostních uhlíkových tkanin (CFRP), Spektrum, 15: 18-21

[13] Benichou N., Kodur V.K.R., Green M.F., Bisby L.A., 2010 Fire Performance of Fibre-Reinforced Polymer Systems Used for the Repair of Concrete Buildings, Construction Technology Update No. 74: 1-6

[14] Ahmed, A., Kodur, V., 2011. The experimental behavior of FRP-strengthened RC beams subjected

to design fire exposure, Engineering Structures, 33: 2201-2211.
DOI: 10.1016/j.engstruct.2011.03.010

[15] Cree, D., Chowdhury, E.U., Green, M.F., Bisby, L.A., Bénichou, N., 2012. Performance in fire of FRP-strengthened and insulated reinforced concrete columns, Fire Safety Journal, 54: 86-95. DOI: 10.1016/j.firesaf.2012.08.006

[16] Argos ®, DBI Jernholmen 12 DK-2650 Hvidovre, DK. http://en.dbi-net.dk/argos/

[17] ISO 834-1: 1999, Fire-resistance tests - Elements of building construction. General requirements. International Standards Organisation, 1999

Article no. 23

THE CIVIL ENGINEERING JOURNAL 4-2015

FIRST STEPS IN URBAN PLANNING OF BULGARIAN CITIES WITH PARTICIPATION OF CZECH ARCHITECTS AND ENGINEERS AT THE TURN OF 19TH AND 20TH CENTURIES

Nikolay Brankov[1]

1. *Czech Technical University in Prague, Faculty of Civil Engineering, Department of Architecture, Thákurova 7/2077, 166 29 Prague, Czech Republic; nikolay.brankov@fsv.cvut.cz*

ABSTRACT

This article focuses on beginnings of the urban planning and first organized planning activities of Bulgarian cities at the turn of 19th and 20th centuries when many Czech engineers and architects participated in significantly. A common feature of all Bulgarian cities was irregular structure and build-up area. The main task of the Czech engineers was to cope with this situation and to design modern cities. In general, the original structure did not make planning easy and unambiguous. Planning of the cities destroyed in the Russian-Turkish war in 1877-78 was easier. A possibility to apply a new city structure freely existed in Stara Zagora and partially in Nova Zagora. A usual principle was straightening of the streets where the engineers used original street network and the new modern streets were built according to it, e.g. the centre of Kystendil and the old part of Nova Zagora. These principles were used also in some central parts of Sofia and Plovdiv. The city of Sofia itself is a distinctive example. Although the original structure was preserved during the war and in the first steps the principle of straightening of the streets in the centre was applied, the other parts of Sofia were designed with a new structure and the old city disappeared. Plovdiv is in contrary to Sofia and its original structure was preserved as an old city and the new one was joined to it in neighbourhoods.

KEYWORDS

Urban Planning; Bulgaria; Czech Architects and Engineers; turn of 19th and 20th centuries; Stara Zagora; Nova Zagora; Sofia; Plovdiv;

INTRODUCTION

This article focuses on the beginnings of an urban planning and first organized planning activities of Bulgarian cities at the turn of 19th and 20th centuries when h many Czech engineers and architects also participated in significantly. The Czech presence became a phenomenon in all cultural fields in Bulgaria at the end of 19th century. Having chosen some illustrious examples, the article tries to make an overview of possible planning principles and attitudes to the original city structure which were applied at that time in Bulgaria. The specific time context requires tracing shortly the distinctive development of the Bulgarian lands and the factors that influenced cultural and social progress in the 2nd half of 19th century in this Balkan country.

METHODS

The followed period and the work of the Czech engineers and architects in Bulgaria have not been researched widely and deeply yet. Some Bulgarian authors have dealt with some of these engineers in their works (e. g. [2] [5] [6] [7] [8] [9] [19]), but nowadays there is no detailed study tracing the work of Czech engineers in Bulgaria. Even in the Czech Republic this topic is known only little. One of the recent attempts was done by an architect David Vávra and his documentary Šumné stopy (2012).

The topic is also the theme of author's PhD. thesis. This article uses historiographical methods based on a heuristic research and includes some new facts discovered during the author's research in Bulgarian and Czech archives.

TIME CONTEXT

In 19th century Bulgarian complicated and dynamic evolution went through. It can be generally divided into two completely different periods. ***The first period*** until 1878 was a part of much larger period called in the cultural history Bulgarian National Revival (or Bulgarian Renaissance). This period was closely linked to the development of Ottoman Empire and Bulgarian land was part of it (1396-1878). The beginning of this period can be found in the 18th century and therefore in the 19th century the main cultural processes culminated. The Orthodox faith and the family as a main social unit, holding together and handling the family memory and traditions over to the younger generations, helped Bulgarian people to retain their national identity. The whole process of Bulgarian National Revival was linked with total national awareness creating stable school system (around 1820-70), obtaining independence of the Bulgarian church from Greek orthodox church (1871) and gaining freedom, which happened in February 1878 as a result of Russian-Turkish war (1877-1878) when Bulgarians could have a free country again.

The second period began after the Liberation and was characterized by the difficult task of building the new state (broadly speaking from the grounds), returning to the European cultural stage, obtaining national uniting of all Bulgarian lands (which never succeeded completely) and political independence (up to 1908). During the first nine months after the Liberation (from February 1878) there was a temporary Russian government in the Bulgarian lands which established the foundations of all Bulgarian state institutions. Shortly after the Liberation the Berliner congress (June 1878) divided freed Bulgaria into the parts where only Bulgarian Principality and autonomous territory of Eastern Rumelia remained free. These lands were developed in the same direction until they united again in 1885. This period can be characterized initially with fluent continuity of Bulgarian traditions and at the same time rapid pace of progress directed to the high level of West European culture and trying to get rid of everything reminding Orient and the time of Ottoman yoke. This led to full leaving of the traditions. After 1878 a lot of foreign specialists came to Bulgaria, a great deal of them was from the Czech lands (at that time a part of Austro-Hungarian Empire). They brought the progressive ideas and tendencies of the European culture and architecture. [1]

MAIN CHARACTERISTICS OF BULGARIAN ARCHITECTURE AND URBAN PLANNING AFTER THE LIBERATION 1878

A new development of architecture began together with the building of the new state. New solid houses, administrative, school and sacral buildings were built. This gradually changed the visual appearance of the Bulgarian cities. But at that time the main task, linked to the development of the architecture, was to plan Bulgarian cities because their development was not subject to any regulation and urban planning principles during the long lasting Ottoman yoke. During the Russian-

Turkish war (1877-1878) many cities and villages were burnt down. The extant ones retained their typical oriental city structure and appearance with the feature of narrow crooked streets (Fig. 1), which were no more satisfactory for the new architecture, as well as for the new social and

economic conditions. So one of the most important tasks of the new state was to organize and solve restoration of the damaged cities and modern planning of survival ones. At the time after the Liberation the first technical offices were established by Russian engineers involved in the planning, but in the first years the planning could begin only in a few cities: the organization of the new institutions was very difficult and the whole process was very slow.

First planning activities (in the cities of Sofia, Plovdiv, Silistra and Rousse) were done by the Russian military specialists who were a part of the Russian army. They were military topographers and engineers, who stayed after the war in the country and helped the temporary Russian government. Later, more active administration began in some cities solving the matter of planning faster. Some of the specialists in this field (particularly engineers and technicians) had stayed in Bulgarian lands even before Liberation and had been involved in designing and building of the so-called railway of Baron Hirsch. After the Russian-Turkish war they continued living and working in Bulgaria. However, there was need of much more specialists and many of them were invited from abroad (mainly from Austro-Hungary, Germany, France, Italy, Russia or neighbour countries as Greece, Serbia, Romania, etc.). Many foreign engineers and architects came to Bulgaria on their own, because the new freed Slavonic country offered a new field for professional work. Statistics show that over 100 foreign specialists worked for first 5-6 years in Bulgaria. The specialists held high and responsible positions such as main city architect or district architect (many of these architects were Czech). These architects solved all questions connected with the building in the city/district as well as the city planning. Another matter was that many specialists were often changed with the new chosen government or municipality and the work started on the planning was stopped, so that the new appointed architect had to start everything from the beginning. Sometimes the ready plan was not realized because of other reasons. [2]

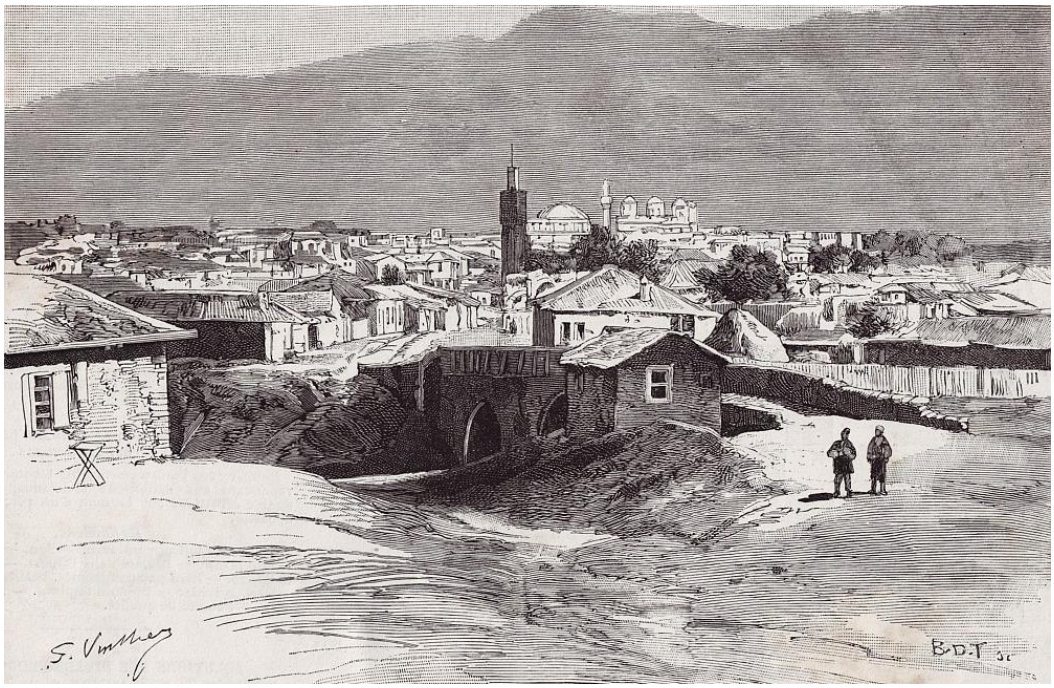

Fig. 1 Typical appearance of the Bulgarian cities after the Liberation: the city of Sofia, old engraving. Source: http://stara-sofia.com/gravsharenmost.jpg

In 1881 ***Rules for construction of private buildings in the cities of Bulgarian Principality*** were approved. They constituted the first legislative document which dealt with matters and principles of city planning. A new requirement of planning was included, that was the geometric principle of city planning (at that time called an „American“ or „European“ way of planning). In autonomous territory of Eastern Rumelia there had not been any legislative documents till 1885, when Eastern Rumelia united with the Bulgarian Principality. First steps in the planning were based on working out a cadastral plan (most of these pictures of the biggest cities were made by Russian topographers during or straight after the Liberation of Bulgaria) and then the architects draw a new regulation of the city streets. This „regulation“ was linked mainly with „straightening“ of the crooked streets and defining the spaces for new public buildings. The complex solving the urban planning including city utility came with a new law in 1897. [2]

CZECH ROOTS OF BULGARIAN URBAN PLANNING

The biggest part of the foreign specialists came from the Czech lands. The Czech presence in all Bulgarian cultural fields became a cultural phenomenon. [3] [4] Czech technicians worked on planning of about 40 Bulgarian cities and towns e.g. Libor Bayer, Josef Boháček, Jeroným Bohutínský, Václav Havrda, Josef Jukl, Bohuslav Kočí, Václav Krásný, Adolf Kolář, Jiří Prošek, Václav Roubal, Josef Schnitter, Karel Trnka etc., who worked out the first cadastral and regulatory plans of a big part of Bulgarian cities and laid the foundations of modern urban planning in Bulgaria. In this article the author has chosen some examples that are different, distinctive and use different planning principles: the plans of the cities of Stara Zagora (1879, Libor Bayer), Sofia (1878-1881, Adolf Kolář, Jiří Prošek and Václav Roubal etc.), Nova Zagora (1880-1883, Libor Bayer), Plovdiv (1888-1892, Josef Schnitter) a Kyustendil (1892, Libor Bayer). [2] [5] [6]

Fig. 2: Original structure of the city of Stara Zagora before the war 1877-1878. Source [2]

The planning of the city of Stara Zagora (1879)

The city of Stara Zagora was totally destroyed during the Russian-Turkish war 1877-1878 and after the Liberation and Berlin Congress it stayed in the territory of Eastern Rumelia. The city needed urgently a new plan to be built again. This plan was made by a Czech architect Libor Bayer within two months.

After the Russian-Turkish war (February 1878) the survived inhabitants came back to the destroyed city. A new municipality had to solve a first problem connected with housing. Some of the families settled in some extant Turkish houses, but all the conditions were dismal. At the beginning of 1879 the number of inhabitants increased dramatically because some of the Turks, who had run away during the war, returned and wanted their own houses. The question of planning the city was very urgent. The main problem was how to solve the ownership of all estates. A special commission evaluated the estates according their state before the war and then all of them were expropriated. Many inhabitants did not want to give their estates but after a lot of city meetings all of them agreed (February 1879). The municipality did not have any specialists so they found a Czech technician Libor Bayer (around 1850-1912) working at that time in the city of Tatar Pazardzhik and invited him to become a city engineer and work out a new city plan. [7] [8] [9]

Fig. 3: Regulatory plan of the city of Stara Zagora by Libor Bayer, 1879.
Source: Regional Historical Museum in Stara Zagora

In April 1879 Libor Bayer arrived with his family to Stara Zagora and he started working on the city plan immediately. Because of the housing crisis there was no time to do any detailed research on the earlier situation of the city and in May the plan was finished. Bayer applied a freely orthogonal geometrical network that did not take into account the old streets and buildings. On 21th of May 1879 the municipality accepted the plan and it was sent to the Directory of public buildings of Eastern Rumelia to be approved. Before approving the director Georgi Valkovich sent the main architect of Eastern Rumelia, the Italian Pietro Montani, to Stara Zagora to check the plan properly in situ. On 2th August 1879 the plan was approved by Montani and then also by the general-gubernator of Estern Rumelia Alexander Bogoridi by decree No. 194 from 27th August 1879. The final plan was finished in scale of 1:4000 (Fig. 3). After a month on 23th September 1879 the basic stone of the new city with memorable plate for future generations was laid down by Alexander Bogoridi. So at last in 1879 the construction of new houses began and in the end of the year there were about 310 new houses. The beginning was very difficult and there were a lot of people without housing and a lot of complainers. But in some time the plan was realized and the city of Stara Zagora turned into a modern European city. [7] [8] [9] [10] [11]

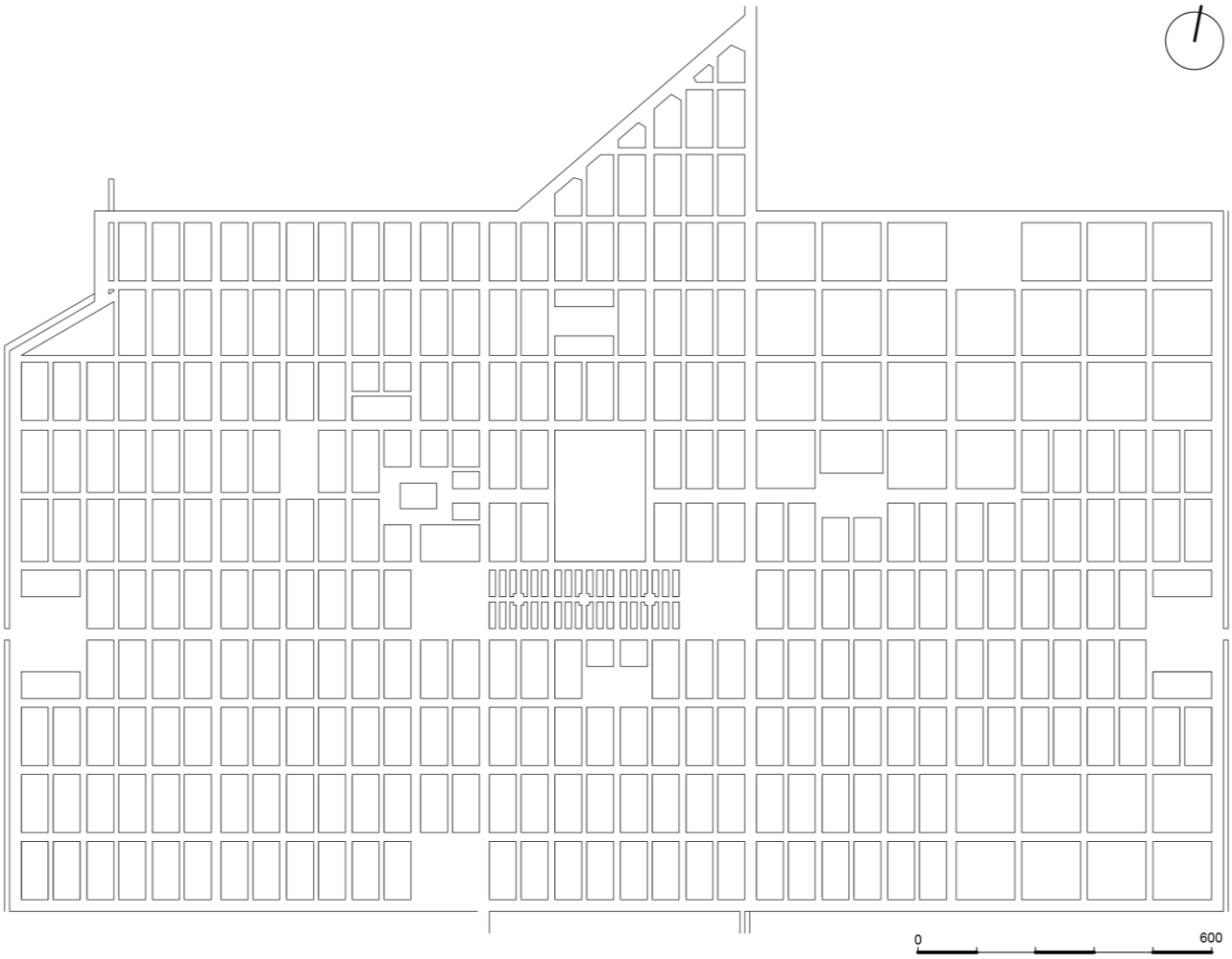

Fig. 4: The new street network according the Bayer's regulatory plan of the city of Stara Zagora, 1879. Source: author

Bayer's plan was worked out in a tersely geometrical way, but it was closer to the planning of the ancient Roman city of Ulpia Augusta Trayana, whose remains lay under the city of Stara Zagora and were exposed during the war. The streets were arranged into a regular orthogonal network and orientated according the four cardinal directions, but with small diversion of 11° in direction North-East and South-West. This brought the city an advantageous South-West position. The streets had three unified widths of 10, 16 and 20 m. The city blocks had also unified 55 m x 120 m with estates with area of 330 m^2 or 660 m^2. Exception were three central blocks in the centre of the city designated for the main shopping street (charshiya) with estates of the shops (dyukyans) with width of 4 or 6 m and depth 7,5 m. In the direction of North-South there were a few streets with a width of 20 m. All streets in the direction East-West were at least 14 m in width and one was 30 m in width with the features of a representative avenue. The plan envisaged enough space for squares, City Park, administrative buildings, schools and churches. Originally there were planned 15 squares, but only 9 have been realised. [7] [8] [9] [10] [11] [12]

Planning of the city of Sofia (1878-1881)

During the Liberation the city of Sofia was a small town (Fig. 5) which was chosen as the capital city of Bulgarian Principality in 1879 and as the seat of all state institutions. In first months after the war Czech engineers worked there. The new city plans gradually changed the old Sofia into a new modern city.

After the war the new municipality dealt with working out a new city plan. On 3th May 1878 the Czech architect Adolf Kolář (1845-1900) was appointed as a main city architect. He had to do all necessary technical works in the city. Kolář began working on the city plan and in the summer 1878 he did research and led the cleaning of the terrain and demolishing of old houses. The plan was finished at the end of the summer, when the first work on the new streets began. This plan does not exist today but we can conclude about it from some reports of municipality from 1878. The plan envisaged new and wider streets and new city parts. However, it did not include the entire city but only its central parts. Therefore, the municipality decided to have a new detailed plan of the whole city been worked. Parallel to the realization of the first Kolář's plan detailed regulatory plans of each city part were worked out according to Kolář's initial plan. [13]

On 10th October 1878 Sofia became the seat of the temporary Russian government in Bulgaria. The Russian emperor's commissar Prince Alexander Dondukov came to Sofia and in a few days approved Kolář's plan. On 25th January 1879 Adolf Kolář was appointed in the department of public building under the leadership of Prince Dondukov. Another Czech - Václav Roubal (1847-1888) was appointed as the main architect of the city. He continued in Kolář's work in the city. [13]

On 22th March 1879 Sofia was proclaimed as the capital city of the Bulgarian Principality (before that time the capital had been the city of Tarnovo, which was the former medieval Bulgarian capital) and in April Prince Alexander Batenberg was proclaimed for the first Bulgarian Prince. By that time the regulatory plans of 6 new quarters had been finished and in May and June another plans were finished: the regulatory plan of square Horse market (by Václav Roubal), Samokovska Street and the regulatory plan of square Rye market (by another Czech engineer Jiří Prošek, 1847-1905). [13]

On 13th July 1879 Prince Alexander Batenberg came to Sofia. A month later after his arrival on 29th August 1879 the ***New regulatory plan of the city Sofia*** combining all partial regulatory plans of all city parts was approved by the Building department of Ministry of the Interior and presented to the Prince. This plan does not also exist today. In the first years after the Liberation the planning of the city of Sofia was done by many Czech architects and engineers: Adolf Kolář,

Václav Roubal, Jiří Prošek (supported by his brother Bohdan Prošek), Jeroným Bohutínský, and also Russian engineers Gette, Bergshtreser etc. According this plan, the first steps in planning were created with building of new streets, demolishing of old houses and constructing of new houses and buildings. [13]

Fig. 5: Original structure of the city of Stara Zagora before the war 1877-1878.
Source: Zheleva-Martins D., 2006. Biografiya na Sofiya

Nevertheless, at the end of 1879 a special commission was chosen for working out a completely new city plan. The Russian engineer Nikolay Kopytkin, former gubernia engineer and later main government engineer, stood in the head of the commission. Václav Roubal was the main city architect till the summer 1880 (than he was a deputy of the main architect Licurgo

Amadey). The new plan was regulatory and it was approved on 10th April 1880. Its main author was an engineer Kopytkin. The plan was later called Batenberg's plan. This plan envisaged wide streets (up to 28 m) and was based on a geometrical network in that time in Bulgaria called "American" combined with ring avenues. Although, it can be considered that Kopytkin based his plan on already finished works during the first two years after the Liberation. His new city plan began to be realised. [13] [14]

From April 1880 Kopytkin and probably also a city architect Licurgo Amadey and his deputy Václav Roubal worked on a cadastral plan of the city of Sofia (till 1881). This cadastral plan was approved on 2th June 1881. At the end a detailed plan combining the Kopytkin's regulatory and cadastral plan was worked out. All the three plans – regulatory, cadastral and detailed (Fig. 6) were approved together on 3th September 1881. The realisation of the plan was going on to the first half of 1890s. [13] [14]

Fig. 6: Detailed (combined) Kopytkin's plan of the city of Sofia, 1881.
Source: Zheleva-Martins D., 2006 Biografiya na Sofiya

The first two city plans - **Kolář's one** and the **New regulatory plan the city of Sofia** does not exist today, but it can be considered that both plans were based on the principle of straightening and broadening the streets. These plans worked with original city structure. The city centre was defined by old important buildings e. g. former Turkish konak (administrative headquarters) later the seat of the Bulgarian Prince Alexander Batenberg, cathedral St. King, city gardens etc. In the city structure there were old important routes (entrance roads to the city), which exist today [13] [14]. **Kopytkin's plan** was based on the principles of radial-concentric cities (such as the system of European metropolis e.g. Vienna's Ringstrasse) combined in inner with geometrical orthogonal networks which did not take into account the old streets and buildings. It is very probable that Kopytkin came out of the first Czech plans in the central parts, in addition he preserved the main city routes leading to the city centre.

Fig. 7: Libor Bayer's regulatory plan of the city of Nova Zagora, 1881. Source: author

Planning of the city of Nova Zagora (1880-1883)

This city, similarly to the nearest Stara Zagora, was destroyed during the Russian-Turkish war. The need of urgent planning forced the municipality of Nova Zagora to look for an engineer who would plan the city. Making of the plan was given to the main city engineer of Stara Zagora Libor Bayer who worked out the city planning in two stages. First he planned the new part of the city southward (before the war the city had hygienic problems) and then he prepared the complex regulatory plan of the city with its old part.

On 21th August 1880 the plan was approved. Bayer's plan included the part between the old city and the railway station which was out of the city to the South. It was only a partial regulatory plan of the city. This plan was approved also by general-gubernator of Eastern Rumelia Alexander Bogoridi on 5th May 1881. But housing crisis led to the decision of the municipality of Nova Zagora to plan the whole city. Bayer worked out a new regulatory plan combining his first one with a new regulation of the old city. This plan was approved on 4th February 1883 (Fig. 7). [11] [15] [16]

The new city part of Nova Zagora was based on the same principles used in Stara Zagora – on an orthogonal network. The city had again a diversion of 11° in the direction South-West and North-East. The old part was based on the principle of straightening and broadening the old city streets. Both, the old and new parts of the city, were delicately joined. The city obtained a peculiar circuit of orthogonal avenues around the city which led to the railway station. The plan envisaged also a few squares and a city park, but nowadays only one city square exists. [11] [15] [16]

Planning of the city of Plovdiv (1888-1892)

The city of Plovdiv was still a big and important city during the Ottoman period with its well preserved original structure. A problem of the city plan was solved at the end of 1880s. The main architect of the city Czech Josef Schnitter was engaged to work out the regulatory plan of the whole city. He preserved the old city structure and designed new city parts in one complex plan.

In 1887 a special wooden pavilion with diameter 8.5 m was built for Schnitter's planning in the City park. Before the planning itself it was important to complete a cadastral survey of the city. The work on geodetic survey took place mainly at night using the lightening from lamps and torches (the truth about this fact is that a lot of inhabitants were against Schnitter and his work, because they thought the new plan could change their estates in the city). The plan was finished between 1888 and 1890 and Schnitter began to work on the regulatory plan. The plan itself was a big plate 6 x 7 m and was laid down on the floor of the wooden pavilion. Josef Schnitter worked dressed in white and clean clothes on this plate, he even wore white socks. The work was very hard and the plan was ready about 1891-92 in scale of 1:500. The plan was approved after some changes in 1896. The original plan was cut into pieces and it exists nowadays in Plovdiv archive. In 1906 the same plan was printed in scale 1:5000 (Fig. 8). [17]

Schnitter's regulatory plan was his ***masterpiece***. He managed to preserve the city history and its architectural authenticity and uniqueness. Schnitter followed maximally the original streets and buildings and the old city structure has been preserved till today. New city parts were designed in a modern way although they honoured the natural, historical and archaeological determinateness (the typical hills, the river). The city got a unique system of four ring avenues orientated according to the four cardinal directions. The new structure was combined with historical routes, including green system and regulation of the Maritsa River. So Schnitter's plan was the first one which preserved unconditionally the old city structure. [17]

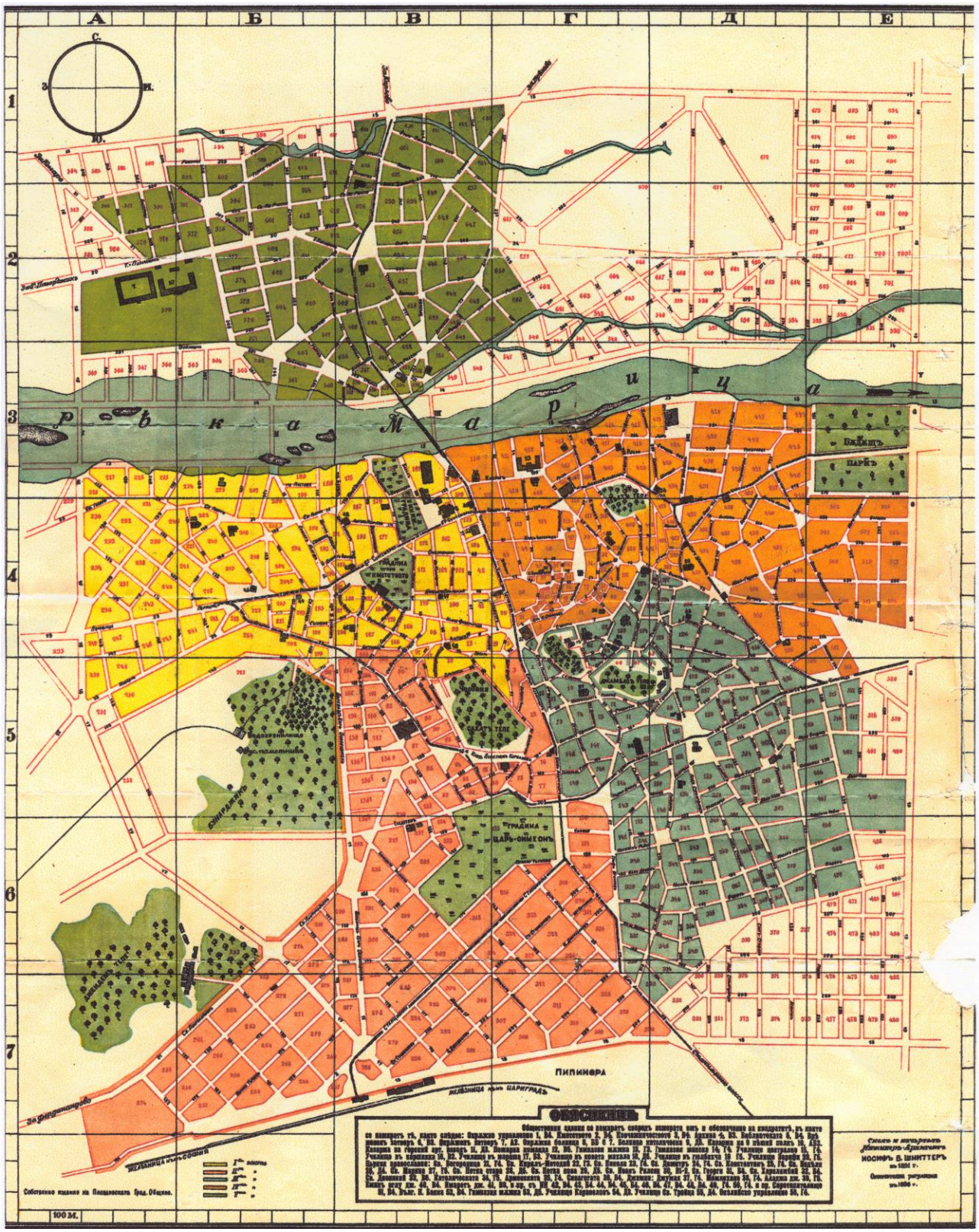

Fig. 8: Josef Schnitter's regulatory plan of the city of Plovdiv (1891-92), print from 1906.
Source: Maria Schnitter

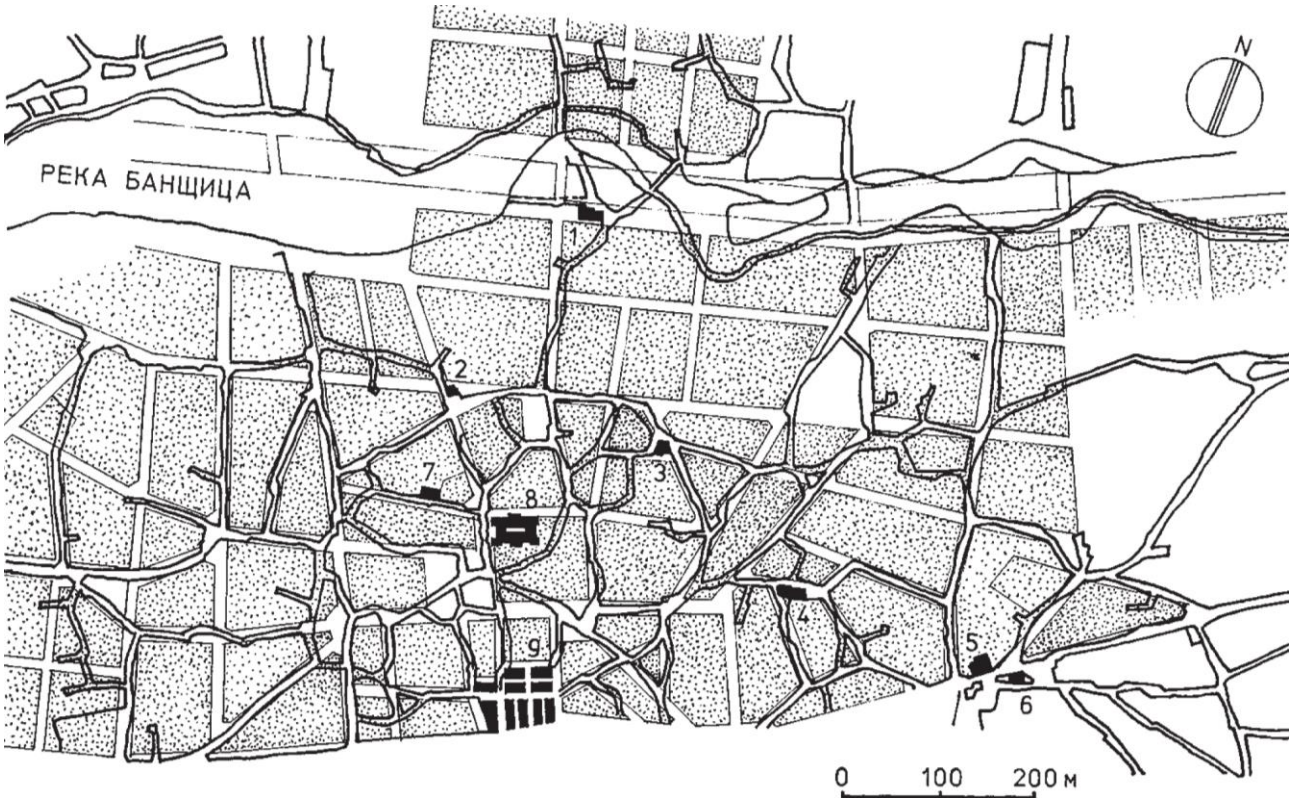

Fig. 9: Libor Bayer's regulatory plan of the city of Kystendil according the heliographic. A copy from 1893. Source [18]

Planning of the city of Kystendil (after 1892)

The city of Kystendil was a small provincial city near the western state borders with preserved city structure. A city plan was worked out by Libor Bayer who became a city architect in 1891.

Libor Bayer finished the plan of Kystendil about 1892 (Fig. 9). According to the contract with the municipality the city had an older plan, probably a cadastral survey. So Libor Bayer had the opportunity to work in this city with its preserved structure. His new plan combined streets around the borders (pomerium) of the ancient city of Pauthalia and the radial-concentric ring system of medieval Kyustendil. New parts of the city were planned in a geometrical orthogonal network. [18]

A main thing in forming of the city centre was the position of the Pedagogical school (1889-1894, on Fig. 10 signed as No. 1) designed by an architect Fridrich Grünanger (1856-1929). A big square 75 x 75 m had arisen next to the school, situated on the same place where the medieval and renaissance square of the city was (Fig. 10). [18]

Libor Bayer preserved the continuity of the public space of the city. Some old streets were preserved only by their straightening and broadening. The plan was realised partially, only the so called Market quarter was established. In 1906 an architect Christo Kovachevski made some changes of the plan, but in 1909 a new regulatory plan designed by an architect Georgi Nenov was approved.

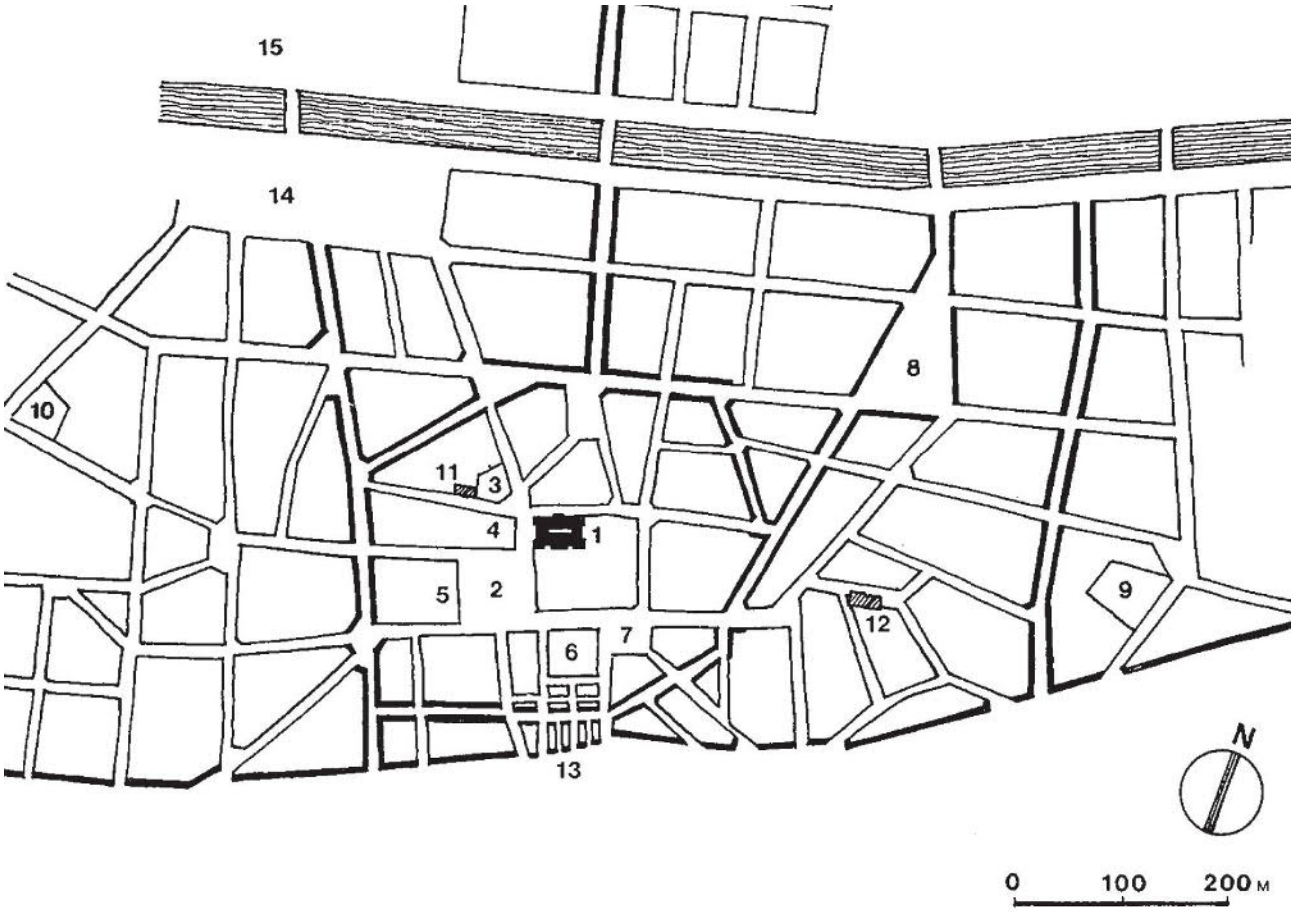

Fig. 10: Libor Bayer's regulatory plan of the city of Kyustendil – main ideas. Source: [18]

CONCLUSION

This article has dealt with different examples of Bulgarian city planning provided by Czech architects and engineers after the Liberation of Bulgaria. Choosing the examples, the aim of this article has been to trace the different planning principles used in Bulgaria at the end of 19th century. As it is shown, the Czech engineers and architects participated in most of described examples.

A common feature of all Bulgarian cities was irregular structure and build-up area. The main task of the Czech engineers was to cope with this situation and design modern cities. In general, the original structure did not make planning easy and unambiguous. In many cases entire historic spaces disappeared under the new changes. The planning of the cities destroyed in the Russian-Turkish war in 1877-78 was easier. A rare example, where the original structure was preserved, is the city of Plovdiv.

Making an overview of the principles the following types of planning can be seen:

- demolished town → new orthogonal city structure – the city of Stara Zagora

- demolished town → „straightening "of the earlier streets, eventually combined with new city orthogonal structure – the city of Nova Zagora

- extant city → straightening of the original streets (with demolishing of old houses), eventually combined with new city structure (orthogonal) –the city of Kyustendil and in the most

of other Bulgarian cities

- extant city → new city structure (orthogonal, radial) – the city of Sofia

- extant city → preserving its original structure combined with new city structure – the city of Plovdiv.

A possibility to apply freely a new city structure existed in Stara Zagora and partially in Nova Zagora. A usual principle was straightening of the streets where the engineers used original street network and according to them the new modern streets were built, e.g. the centre of Kystendil and the old part of Nova Zagora. These principles were used also in some central parts of Sofia and Plovdiv. Although many old historical buildings and houses were knocked down, the original street network was partially preserved. After 1881, when *Rules for constructing private buildings in the cities of Bulgarian Principality* were approved, every new part of the city had to be founded on regular orthogonal network (by „American“ way). It is seen in the city plan of Kjustendil, Nova Zagora and Plovdiv. The city of Sofia itself is a distinctive example. Although the original structure was preserved during the war and in the first steps principle of straightening of the streets in the centre was applied, the other parts of Sofia were designed with a new structure and the old city disappeared. These examples are close to other European cities such as Paris, Prague and Vienna. Plovdiv is in contrary to Sofia and its original structure was preserved as an old city and the new one was joined to it in neighbourhoods.

To sum up, the first steps of planning of Bulgarian cities were connected with the conflict of old-new, but the contribution of foreign mainly Czech architects is undeniable. Many new regulatory plans enabled a new development of long-lasting stagnating Bulgarian cities and at the end of 19th century a new page in the history of architecture and urban planning in Bulgaria was opened.

ACKNOWLEDGEMENTS

This work was supported by the Grant Agency of the Czech Technical University in Prague, grant No. SGS 15/135/OHK1/2T/11.

REFERENCES

[1] Martínek J., 2009. Bulharsko. (Nakladatelství Libri, Praha). 136 s.

[2] Avramov I., 1957. Planiraneto na naselenite mesta v Bălgarija ot Osvobožđenieto do 9 septemvri 1944 god.: Istoričesko-gradoustrojstven očerk. Izvestija na instituta po gradoustrojstvo i architektura. Kniga deseta i edinadeseta, Materiali ot istorijata na bălgarskata architektura, 389-456

[3] Strohsová K., 2012. Migrace Čechů do Bulharska – tzv. „česká invaze“. Antropowebzin (online), vol. 8, issue 1: 32-37. Available from: http://antropologie.zcu.cz/media/document/art_6_strohsova.pdf (cit. 8.6.2014)

[4] Urban Z., 1981. Chehi i balgari: kulturni vzaimootnosheniya (Izdatelstvo na Otechestveniya front, Sofia) 228 s.

[5] Doychinov G., Ganchev H. a Stoyanova I., 2002. Balgariya - 1900: Evropeyski vliyaniya v balgarskoto gradoustroystvo, architektura, parkove i gradini 1878-1918 (Arhitekturno izdatelstvo Arh & Art, Sofia) 266 s.

[6] Doytchinov G., Gantchev Ch., 2001. Österreichische Architekten in Bulgarien: 1878-1918. (Böhlau

Verlag, Wien) 228 S.

[7] Doneva V., 2012. Na gazena lampa razchertali plana za opozharena Stara Zagora. PressaDaily (online), 13th November 2012. Available from: http://pressadaily.bg/publication/5836-На-газена-лампа-разчертали-плана-за-опожарена-Стара-Загора/#void (cit. 12.1.2014).

[8] Coneva R. et al., 2007. Vazstanovyavane na grad Stara Zagora - istoricheski belezhki za deynostta na Libor Bayer = Reconstruction of Stara Zagora - historic memorandum of Libor Bayer's activities. In: Meždunarodna naučna konferencija, Stara Zagora - 2007, 7 - 8 juni 2007. Tom V, Obštestveni nauki. Istorija, Bălgarski ezik i literatura. Bogoslovski nauki = International science conference, Stara Zagora - 2007, 7th - 8th June 2007. Volume V, Social studies. History, Bulgarian Language. Theological Studies (Izdatelstvo Sayuz na uchenite, Stara Zagora), 181-185.

[9] Coneva R. et al., 2009. Deloto na Libor Bayer - tradiciya i priemstvenost v Profesionalna gimnaziya po stroitelstvo, architektura i geodeziya - Stara Zagora = Libor Bayer's work - a tradition and continuity in Polytechnic school of architecture, civil engineering and geodesy - Stara Zagora. In: *Meždunarodna naučna konferencija "Razvitie na ikonomikata i obštestvoto na osnova na poznanieto", Stara Zagora, 4 - 5 juni 2009.* Tom VI, Obštestveni nauki. Istorija = *International Science conference "Economics and Society development on the Base of Knowledge", Stara Zagora, 4th - 5th June 2009.* Volume VI, Social studies. History. (Izdatelstvo Sayuz na uchenite, Stara Zagora), 64-68.

[10] Dimitrova S., Marinova S., Vasileva S., Nikolova M. Na tozi den...: 130 g. ot života na Stara Zagora. (Izdatelstvo Lagen, Stara Zagora) 228 s.

[11] Zheleva-Martins D., Farkov Y., 2009. Istoriya na balgarskoto gradoustroystvo prez 19-20 vek. Parva chast, Diachronni analizi, Chapter Gradoustroystvena evolyuciya na grad Stara Zagora (ot vaznikvaneto na selishteto do sredata na XX vek). (Izdatelstvo Valentin Trayanov) 86-115 s.

[12] Koycheva V., 1980. Parviyat regulacionen plan na Stara Zagora. Muzei i pametnici na kulturata, vol. 20, issue 3: 16-20

[13] Zheleva-Martins D., 2006 Biografiya na Sofiya: Istoricheski studii, Chapter 120 godini ot parviya regulacionen plan na grad Sofiya (Izdatelstvo Prostranstvo-forma, Sofia), 51-56

[14] Zheleva-Martins D., 2006 Biografiya na Sofiya: Istoricheski studii, Chapter Gradoustroystveno planirane i istoricheski kontext (Izdatelstvo Prostranstvo-forma, Sofia), 57-68

[15] Nikolova, P., 2009. Kmet zhertva istoricheski ploshtad zaradi hotel. Desant na patriotichniya pechat - nacionalen sedmichnik (online). Available from: http://www.desant.net/show-news/19681/ (cit. 12.1.2014)

[16] Rusev, Sh., 2009. Istoricheska spravka za centralniya gradski ploshtad "Svoboda" i pametnika "Zagorci" v Nova Zagora. Nova Zagora - tova e našijat grad (online). Available from: http://novazagora.com/forum/viewtopic.php?id=94&p=5 (cit. 12.1.2014)

[17] Brankov N., 2014. Josef Schnitter - tvůrce moderního Plovdivu. EARCH (online), 12th May 2014. Available from: http://www.earch.cz/cs/revue/josef-schnitter-tvurce-moderniho-plovdivu (cit. 26.5.2014)

[18] Zheleva-Martins D., Farkov Y., 2009. Istoriya na balgarskoto gradoustroystvo prez 19-20 vek. Parva chast, Diachronni analizi, Chapter Gradoustroystvena evolyuciya na grad Kyustendil (ot vaznikvaneto na selishteto do sredata na XX vek) (Izdatelstvo Valentin Trayanov, Sofia), 244-273

Article no. 24

THE CIVIL ENGINEERING JOURNAL 4-2015

INFLUENCE OF CYCLIC LOADING ON THE DEFLECTION DEVELOPMENT OF CONCRETE SPECIMENS

Marek Foglar[1] and Jakub Göringer[2]

1. *Czech Technical University in Prague, Faculty of Civil Engineering, Department of Concrete and Masonry Structures, Thakurova 7, Prague 6, Czech Republic; marek.foglar@fsv.cvut.cz*
2. *Czech Technical University in Prague, Faculty of Civil Engineering, Department of Concrete and Masonry Structures, Thakurova 7, Prague 6, Czech Republic; jakub.goringer@fsv.cvut.cz*

ABSTRACT

Durability of the structures is one of the most discussed issues of last decades. It is one of the most easily measured properties for analysis during the structural lifetime. Concrete deflections increase over time due to rheological effects (creep and shrinkage) in addition cyclic creep can be observed on the cyclically loaded structures. The deflection increase due to the cyclic creep is not properly quantified. The fatigue damage function presented in this paper provides an analytical solution for the deflection development due to cyclic loading. The evaluation of the deflection is based on the reduction of the initial modulus of elasticity.

Main principles of the function are discussed and compared with the standardized approaches for the fatigue assessment. Experimental verification of the fatigue damage function was carried out on reinforced concrete specimens and on prestressed concrete slab. To improve the standardized approaches, the real stress distribution was considered with the use of newly-developed method of partial integration over the height of the specimen compressive zone.

The deflection increase due to cyclic loading was measured regularly with inductive displacement transducer. Comparison of the measured values and the values calculated using the presented function shows good agreement. The fatigue damage function can be used easily in “in-hand” calculations, or can be inserted into FEM-based software and used in practical applications for assessing the increase in the deformations of concrete structural elements caused by cyclic loading.

KEYWORDS

Concrete, fatigue, cyclic loading, strain, deflection, experimental methods

INTRODUCTION

Fatigue is commonly defined as a process of permanent progressive changes in the structure of a material exposed to cyclic loading. Concrete is nowadays one of the most widely-used building materials for various kinds of structures. Along with the improvements in its properties, the use of high strength concrete has resulted in the design of slenderer structures. These structures are subjected to a higher live load proportion of the total load, and greater

vulnerability to fatigue failure can therefore be assumed. Many common structures, bridges and crane tracks are exposed to cyclic loading, which can result in accelerated crack propagation, greater deflections, reduction in structural stiffness and consequently fatigue failure.

Fatigue of concrete and concrete structures was first described at the beginning of the 20th century, and became a significant topic in the 1920s with the development of highways, concrete railway bridges and airport pavements.

History of fatigue of concrete

The first publications dealing with fatigue of concrete came from German authors [1, 2]. These publications were focused on concrete bridges and airport pavements, structures which had to resist 10^5-10^7 load cycles during their lifetime. According to present terminology, this phenomenon is called high-cycle fatigue. In the late 1950s, research was focused mainly on fatigue caused by seismic loading (10^0-10^3 loading cycles). This phenomenon is called low-cycle fatigue. With the rapid growth of mass transport structures in the 1970s, the number of cycles that structures have to resist increased to about 10 to 50 million load cycles.

Fatigue testing of concrete was mainly developed in the 1960s, e.g. [3], with the goal of providing a proper description of the stress-strain curve of concrete exposed to cyclic loading. In the late 1970s, Holmen [4] focused his research on strain development under cyclic loading with different amplitudes.

The developments in concrete fatigue testing show similarities with the developments in static testing of concrete. These studies were performed as compressive tests. They were followed by testing the fatigue of concrete in tension [5], fatigue under varying loads [6] and frequencies [7], and fatigue in flexure [8].

Nowadays, testing in flexure is the most popular type of test, together with biaxial or triaxial compression [9]; the fracture mechanics approach is now widely used in fatigue of concrete.

During the 20th century, many different approaches for fatigue analysis of concrete structural elements were proposed. Hsu [10] extended the S-N curve to the S-N-T-R system, which takes into account the time of loading and the ratio of the minimum and maximum stress applied to the strength of the concrete. Petryna [11] developed a method for assessing the reliability of reinforced concrete structures subjected to fatigue loading. Material models of concrete subjected to cyclic loading are often based on fatigue damage accumulation and micro-crack propagation. Horii [12] pointed out that the fatigue crack initiation mechanism and crack growth are different for static and fatigue loading. This section should describe in detail the study material, procedures and methods used.

The presented paper is focused on the deflection increase due to compressive fatigue of concrete. Influence of the tensile fatigue was neglected due to crack development in reinforced concrete specimens. For the deflection calculation of prestressed specimen the tensile fatigue was simplified as stated in the text.

STRAIN DEVELOPMENT UNDER CYCLIC LOADING

The concrete failure mechanism and strain development under cyclic loading

Concrete is a heterogeneous three-phase material. It is full of flaws and initial stress concentrations, and the fatigue process in this kind of material is much more complex than in homogeneous ferrous materials. The development of the secant modulus of elasticity in concrete subjected to cyclic loading, the cyclic creep curve, consists of three phases as can be seen in Figure 1. Phase 1 - the initiation phase; microcracks develop in the weaker parts of the cement paste and the strain increases rapidly (5-10% of the limit number of applied cycles *N*).Phase 2 - the cracks propagate in a stable manner, and the strain increases approximately linearly with the number of

applied load cycles (about 80% of *N*). Phase 3 - represents unstable crack growth, which leads to fatigue failure of the specimen (remaining 10-15% of *N*).

Development of the secant modulus of concrete under cyclic loading

The development of the secant modulus of elasticity under cyclic loading reflects the development of strain or deformation, and vice-versa. The development of the secant modulus of elasticity under cyclic loading was described by Holmen in 1979 [4], see Fig. 1.

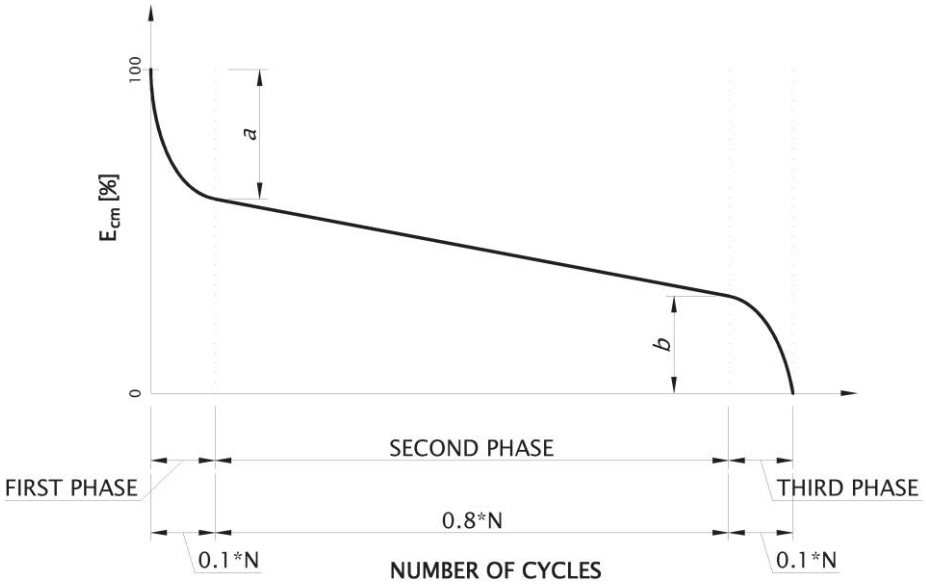

Fig. 1: Development of the secant modulus of elasticity of concrete under cyclic loading [4]

In his research, Holmen used a loading frequency of 5Hz and minimum stress equal to 0.05f_{cm}. The maximum stress varied from 0.675f_{cm} to 0.95f_{cm}. The first phase of development of the secant modulus of elasticity finished at 75-95% of E_{cm}, and the second phase finished at 68-75% of E_{cm}, depending on the maximum stress applied, see Fig. 2.

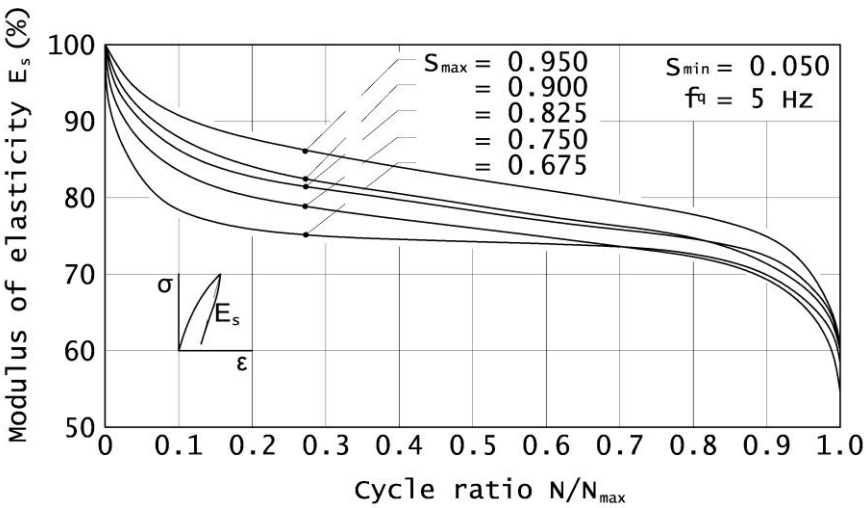

Fig. 2: Percentage reduction of the secant modulus of elasticity with the cycle ratio. Mean curves for different stress levels (from [4])

Parametric description of the secant modulus development under cyclic loading

A parametric description of the development of the secant modulus of elasticity of concrete under cyclic loading is proposed on the basis of experiments carried out by Holmen [4]. These experiments were performed on concrete probe cylinders with dimensions of 100x250 mm (diameter x height) subjected to cyclic compressive loading.

For the purposes of parameterization, the duration of the first phase and also the third phase of the strain development is assumed to be 10% of the total number of load cycles that the structural element is able to resist. Simultaneously, according to the Holmen experiment [4] the contribution of the first and the third phase of the development was substituted by constants for the given compressive stress level S_{max}. $S_{\max}$ is the maximum stress level defined as the ratio between maximum compressive stress and design fatigue endurance $f_{cd,fat}$, as in eq. (1). Coefficient η_c is the averaging factor of concrete stresses in the compression zone considering the stress gradient and it applies only in case of Model Codes [13, 14].

$$S_{\max} = \eta_c \left|\sigma_{c,\max}\right| / f_{cd,fat} \tag{1}$$

$$f_{cd,fat} = \beta_{cc,sus}\left(t,t_0\right)\beta_{cc}\left(t_0\right) f_{cd}\left(1-\frac{f_{ck}}{250}\right) \tag{2}$$

Constants *a* and *b* are introduced, *a* for the decrease in the secant modulus of elasticity in the first phase of its development under cyclic loading, *b* for the remaining proportion of the original secant modulus of elasticity at the beginning of the third phase of its development. The graphical meaning of the constants is explained in Figure 1. The phenomenon of the deflection increase can be as well assumed for structural elements which are exposed to cyclic bending, as described further in this text. The formulas for constants *a* and *b* were obtained by linear regression:

$$a = 0.47 - 0.4S_{\max} \tag{3}$$

$$b = 0.57 + 0.17S_{\max} \tag{4}$$

Due to the method used for assessing the formulas, and input data based on higher stress levels, the formulas for constants *a* and *b* are valid only for stress levels $S_{\max} > 0.174$. For stress levels $S_{\max} < 0.174$ the increase in deflections due to fatigue loading can be neglected, or data from the research carried out by Holmen [4] can be extrapolated. Holmen dynamically tested 462 specimens, thus the dependence of the constants only on stress level $S_{\max}$ based on his research can be considered as correct.

Fatigue damage function

Formulation of the problem, motivation

A mathematical function for describing the strain development in a concrete specimen under cyclic loading is sought for. This function should be able to give a decreasing multiplier of the initial modulus of elasticity at each particular moment of the cyclic loading (after n_i loading cycles), thus respecting the three phases in strain development under cyclic loading. The reduced value of the initial modulus of elasticity can then be used for calculating deflections increased by damage accumulation caused by cyclic loading.

Boundary conditions, simplifications, our approach

The fatigue damage function uses the parametric description of the development of the secant modulus of elasticity of concrete under cyclic loading, as proposed above.

Some further assumptions are added and listed:

- The function is set up (on the x-axis) to the ratio of the number of load cycles that the structural element has already resisted (n) to the total number of load cycles that the structural element is able to resist at the particular load level (this value can be calculated by procedures given e.g. in Eurocode 2 [15] or in the Model Codes [13, 14]).
- The value of the fatigue damage function after the end of the first phase of strain development is equal to (1-a).
- The value of the fatigue damage function at the start of the third phase of strain development is equal to b.

According to the chosen form of the fatigue damage function, the function is the sum of a power function and an exponential function.

Power part of the fatigue damage function

The power part represents the rapid decrease in the modulus of elasticity at the start of cyclic loading, i.e. the first phase of cyclic loading, and the stable progressive decrease in the modulus of elasticity during the majority of the service life of a structural element subjected to cyclic loading, i.e. the second phase of cyclic loading.

The result of the power part has to fulfil the following criteria:

- Its value at n/N = 0.1 has to be equal to a.
- Its value at n/N = 0.9 has to be equal to (1-b).
- Due to the variation in differences between (1-b) and a for various load levels, which determines the increase of the function between n/N = 0.1 and n/N = 0.9, the power has to be a function of S_{max}. The power part of the fatigue damage function can be followed in Fig. 3.

Exponential part of the fatigue damage function

The exponential part is independent of S_{max}. It represents the rapid decrease in the modulus of elasticity at the end of the service life of a structural element (third phase).

The result of the exponential part of the function has to fulfil the following criteria:

- Its value for n/N = 0.0 to 0.9 has to be insignificant.
- Its value for n/N = 0.9 to 1 has to be dominant.
- Its value at n/N = 1 has to be equal to b, so that the sum of the power and exponential part is equal to 1. The exponential part has behaviour as in Fig. 3.

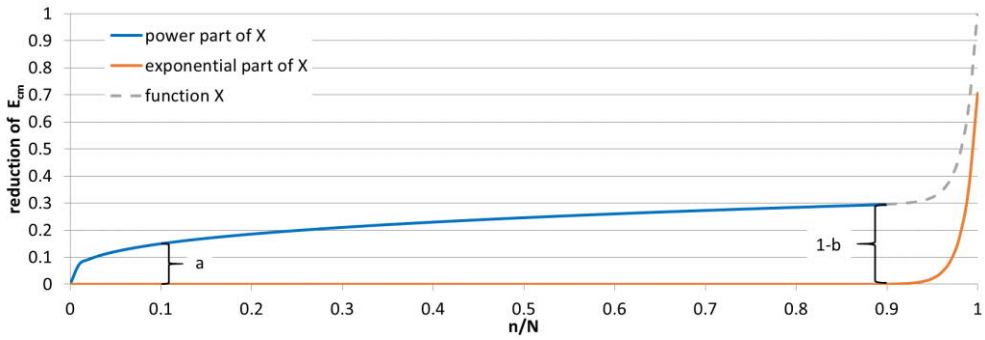

Fig. 3: Example of the power and exponential part of function X

Limit number of applied cycles N – usage and discussion of standards

EN 1992-1 [15] states that the fatigue should be evaluated in the most stressed fibres. Model Code 2010 [13] partially reflects the stress distribution in compression zone with η_c coefficient. Experimental results show that the calculated design values of the limit number of applied cycles *N* according to these standards differs significantly (eq. 5 for Model Code 2010 and eq. 6 for EN 1992-2).

$$\log N_1 = \frac{8}{Y-1}\left(S_{c,\max} - 1\right)$$
$$\log N_2 = 8 + \frac{8 \cdot \ln(10)}{Y-1}\left(Y - S_{c,\min}\right) \cdot \log\left(\frac{S_{c,\max} - S_{c,\min}}{Y - S_{c,\min}}\right) \tag{5}$$

with

$$Y = \frac{0.45 + 1.8 \cdot S_{c,\min}}{1 + 1.8 \cdot S_{c,\min} - 0.3 \cdot S_{c,\min}^2}$$

(a) if $\log N_1 \le 8$, then $\log N = \log N_1$

(b) if $\log N_1 > 8$, then $\log N = \log N_2$

$$\log N = \left(14 \frac{1 - S_{c,\max}}{\sqrt{1 - \sigma_{c,\min} / \sigma_{c,\max}}}\right) \tag{6}$$

Experimental testing of reinforced concrete specimens (described further) did not show any visible damage after 400 thousand cycles, this may correspond with the value of N calculated according to Model Codes – N = ~1.3*10^7, whereas for the calculation according the Eurocode the limit number of applied cycles N = 1900 (both values were calculated using material safety factor γ_M = 1.0). Based on these findings the Model Code is used in the proposed model.

For the evaluation of the prestressed specimen in the experiment the limit number of applied cycles for concrete in tension or in compression-tension were used as in Model Code 2010 [13].

$$\log N = 9\left(1 - S_{c,\max}\right) \quad \text{for } \sigma_{ct,\max} \le 0.026\left|S_{ct,\max}\right|$$
$$\log N = 12\left(1 - S_{ct,\max}\right) \quad \text{for } \sigma_{ct,\max} > 0.026\left|S_{ct,\max}\right| \tag{7}$$

The fatigue damage function

The development described in previous sections leads to the following formulation of the fatigue damage function (eq. 8). Fig. 4 gives an example of the fatigue damage function for various load levels.

$$\omega_{F_i} = 1 - \left\{ a \cdot \left(\frac{n_i}{c_1 N} \right)^{\frac{S_{\max}{}^{c_3}}{c_4}} + b \cdot \exp\left[\left(\frac{n_i}{N} - 1 \right) \cdot c_2 \right] \right\} \tag{8}$$

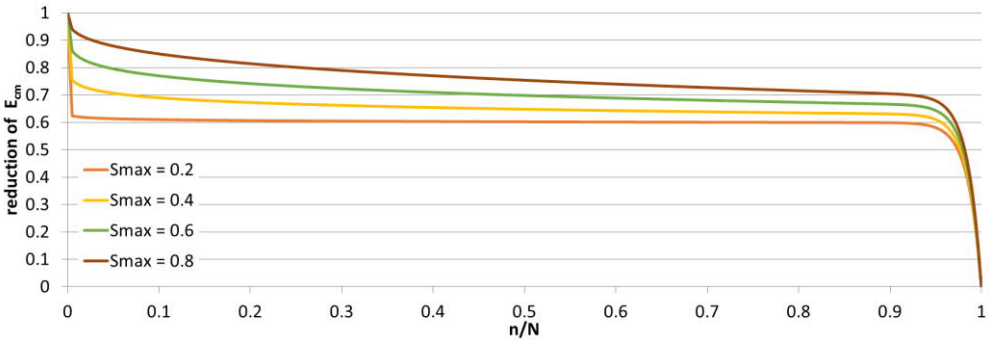

Fig. 4: Example of the fatigue damage function for various load levels

As stated above, the increase in the deflections caused by cyclic loading can be as much as 40% of the initial static deflections. This phenomenon should be taken into consideration especially in evaluating the deflections of existing structures by means of a repeated load test when assessing their remaining useful lifetime (for example bridges with the loading test at the start of the operation, common practice in some countries e.g. the Czech Republic).

With regard to the number of samples tested by Holmen and limitations of described approach only for macro-scale fatigue assessment other factors influencing modulus of elasticity (material texture, porosity etc.) are neglected.

EXPERIMENTAL VERIFICATION OF THE FATIGUE DAMAGE FUNCTION ON REINFORCED AND PRESTRESSED CONCRETE ELEMENTS

General approach to the experimental program with respect to its applicability to real structures

Two types of concrete specimens were prepared for an experimental verification of the fatigue damage function: reinforced concrete specimens and a pre-stressed concrete specimen. The two types are described in the following sections. The preliminary results were presented in [16] and [17]. The results presented here have been widened and evaluated using a new alternative approach for fatigue assessment.

Test arrangement specifications

The four-point bending tests were chosen for their advantage of zone subjected to pure bending (decomposed to pure compression/tension) without the influence of shear. This material point zone, i.e. the crack localization zone corresponds to the behaviour of common structures. The principle described above and the stress distribution on an ideal cross-section is illustrated in Fig. 5.

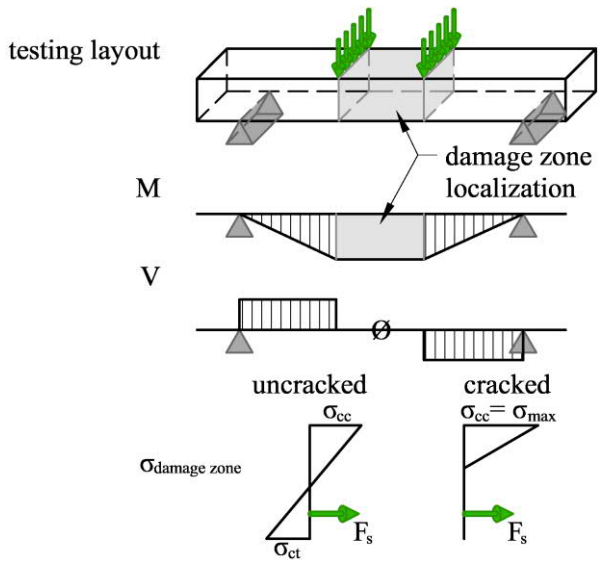

Fig. 5: Four-point bending arrangement and localization zone principle with the stress distribution in the damage zone

Evaluation of the variously stressed fibres of the cross-section

The stress distribution in the calibration experiments [4] was constant, so that each part of the cylinder was exposed to the same conditions. This assumption is not valid for specimens subjected to bending, where each part of the cross-section is exposed to a different compressive or tensile stress. It can be assumed that most of the structures subjected to cyclic loading are exposed to bending.

Dividing the compressive zone over the height of the cross-section was therefore chosen to include a different behaviour of variously stressed fibres, thus presenting a new and less conservative approach to fatigue assessment of a structural element subjected to bending. The analysed cross-section decomposes into an ideal cross-section of layers with a different modulus of elasticity depending on the stresses that it is subjected to. This approach should reflect the differences between the fatigue behaviour of the compressive cyclic loading of the cylinders, which the fatigue damage function is based on, and specimens subjected to cyclic bending.

Calculation of the deflections

For an evaluation of the deflections, partial integration over the compressive zone height was used to reflect the real stress distribution. The method used here is based on the average stress in each layer, and not on the maximal stress in the top fibres, as e.g. in Eurocode 2 [15]. The compressive zone of the cracked concrete specimens was divided into 20 layers (in the case

of 300x150x1300 specimens, each layer has about 3 mm in thickness). This division was based on a sensitivity analysis.

Using coarse division, up to 5 layers, the small average stresses in the wide integration layers lead to results on the unsafe side (in contrast with the standardized approaches). The calculated deflections did not show good agreement with the measured values, and were distinctly lower than the measured values.

With a finer division, up to 15 layers, the average stresses in the layers are higher (and correspond more to the real stresses). Thus some of the layers may exceed the limit number of applied cycles, which leads to a significant reduction in the modulus of elasticity (see below). The division is still coarse, and the height of the layer represents a considerable part of the cross-section. This significantly influences the ideal moment of inertia of the cross section, which may lead to the very conservative results.

Dividing the compressed zone of the ideal cross-section into 20 layers proved to be the optimal solution for these experimental settings. Finer division into more than 20 layers is not necessary, as the difference in the results is negligible in comparison with the possible increase in computational time requirements.

In the comparison of the calculated and measured data (Figure 9 – Figure 12), which will be discussed later, instant increases in the calculated deflections can be observed. This phenomenon is caused by the incorporation of the differences in fatigue behaviour between probe cylinders and beams in bending into the evaluation. From the definition of the fatigue damage function, the modulus of elasticity decreases to zero at the limit number of applied cycles N (this corresponds to the behaviour of the probe cylinders). In the case of cylinders, the specimen fails as a whole element after N cycles; but in the case of specimens subjected to bending, the bond between differently stressed neighbouring parts will influence the behaviour of the specimen. When one layer reaches the limit number of load cycles corresponding to the applied S_{max}, there is still a bond with the neighbouring part. When one of the layers deteriorates, the other layers take over its role. Due to this stress redistribution, some residual values of the modulus of elasticity of the extremely damaged part can be assumed. The position of the neutral axis changes with the deterioration of the layers, and thus changes the maximum stress applied to the layer.

To include the facts mentioned above, the constant multiplier of the modulus of elasticity is used when the fatigue damage function reaches the third phase according to Figure 1. This constant multiplier was taken as an average value of the fatigue damage function at the start of the third phase of the strain development, where the function takes values between approximately 0.65 and 0. Thus the modulus of elasticity value is 0.33 ($E_{residual} = 0.33*E_{cm}$) for $S_{max} \geq 0.2$. For low maximum stresses, it can be assumed that the influence of fatigue is lower. For that reason, the upper limit value of the fatigue damage function ($\omega = 0.65$) was chosen for $S_{max} < 0.2$ ($E_{residual} = 0.65*E_{cm}$). These instant changes in modulus of elasticity lead to instant increases in the calculated deflections, as was mentioned above (Fig. 9 – Fig. 12).

The principle of partial integration described above, and the use of different modulus of elasticity for calculating the ideal moment of inertia, is illustrated in Fig. 6.

In order to calculate the deflections, the ideal moment of inertia is needed. An evaluation of this cross-sectional characteristic was carried out in 4 steps:

1) From the fatigue analysis, the maximum stress levels S_{max} were obtained for each partial height (layer) within each specimen.
2) The fatigue damage function was evaluated depending on the maximum stress levels S_{max}.
3) The decreased modulus of elasticity was calculated with the fatigue damage function for each layer.

4) The ideal moment of inertia was calculated on the basis of the decreased modulus of elasticity of each layer.

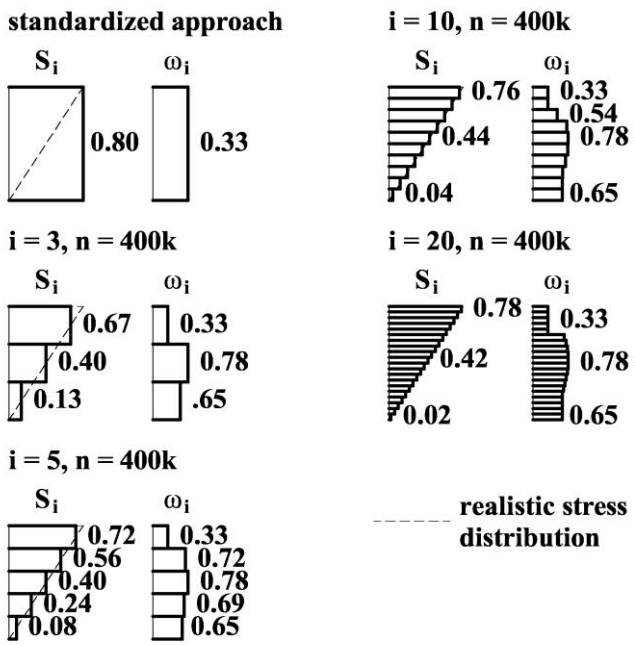

Fig. 6: Principle of partial integration of the compressive zone with the results of sensitive analysis for n = 400,000 cycles

Reinforced concrete specimens

Several sets of specimens were prepared for an experimental verification of the fatigue damage function on reinforced concrete. Each set contains a specimen for cyclic loading (300x150x1300 mm), specimens for evaluating the modulus of elasticity of concrete, tensile strength in bending and compressive strength (100x100x400 mm), and additional 150 mm probe cubes for evaluating the compressive strength.

All specimens were made with concrete strength class C25/30 (for the mix proportions, see Table 1**Chyba! Nenalezen zdroj odkazů.**). The specimens proposed for cyclic loading were designed as over-reinforced (6Ø16 grade B500 reinforcing steel). Thus failure by compressive-zone crushing should occur and fatigue failure of the concrete can be assumed. The scheme of the dimensions and the reinforcement of the specimen is shown in Fig. 7.

Tab. 1: Mix proportions of the concrete mixture

Constituent	**kg/m3**
CEM II 32.5	320
Sand	836
Fine aggregate	495
Coarse aggregate	443
Water	185

w/c ratio	0.58

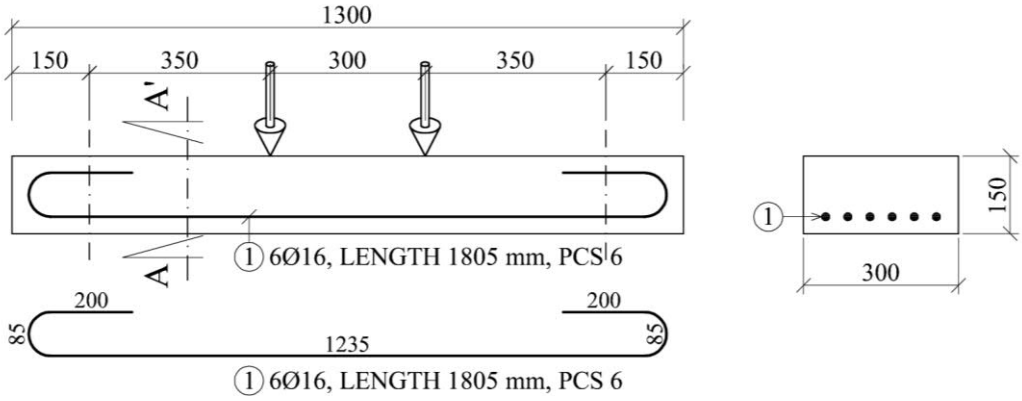

Fig. 7: Scheme of the fatigue testing specimen and its reinforcement

Testing layout

The arrangement of the cyclic loading is four-point bending with a span length of 1000 mm and overhangs 150 mm in length. This testing layout was chosen because it offers several advantages, as discussed in the previous sections. The experiments were conducted in the Experimental Center of the Faculty of Civil Engineering, Czech Technical University in Prague. The parameters of the fatigue testing are presented in Table 2. The arrangement is shown in Fig. 8.

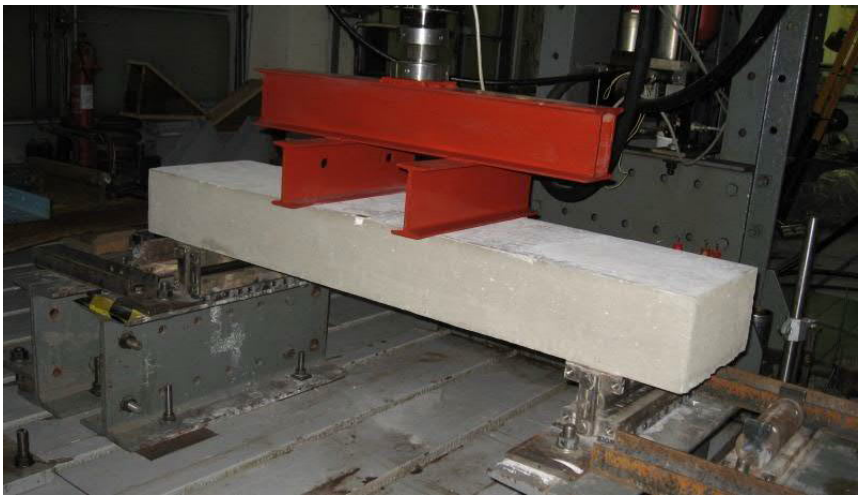

Fig. 8: Arrangement of the fatigue testing

Tab. 2: Specification of the fatigue testing settings

Loading frequency	Cyclic force		Eccentricity
	min	max	
Hz	kN		m
5	5	100	0.3

Deflection measurements and loading history

Two types of deflection measurements were performed during the fatigue testing. The first type - static deflection measurements - takes place after every hour of cyclic loading (circa 18000 load cycles). The second type - dynamic deflection measurement - was carried out during the fatigue testing immediately after the static deflection measurements. In order to obtain the exact deflection in the middle of the span, the settlement of the supports was also measured.

Each specimen was tested for one week, which corresponds to about 350-450 thousand cycles.

The deflections of the reinforced concrete specimens were measured by the inductive displacement transducer. Table 3 presents the measured deflections and the number of load cycles which they were measured at.

Tab. 3: Deflection measurements on reinforced concrete specimens

Specimen #							
1		**2**		**3**		**4**	
Age	32 days	**Age**	61 days	**Age**	29 days	**Age**	64 days
Test. date	21.9.2009	**Test. date**	20.10.2009	**Test. date**	24.9.2013	**Test. date**	29.10.2013
n_i	δ_i [mm]	n_i	δ_i [mm]	n_i	δ_i [mm]	n_i	δ_i [mm]
0	1.094	0	1.177	0	2.015	0	1.343
28080	1.334	7760	1.125	78772	1.730	18250	1.216
40440	1.406	14960	1.202	78772	1.380	40398	1.287
60930	1.654	21820	1.228	138225	1.404	54442	1.348
90450	1.514	40040	1.275	197512	1.393	68644	1.371
90450	1.511	60120	1.297	197512	1.400	83847	1.380
110560	1.576	60120	1.314	249298	1.406	92780	1.383
110560	1.562	78330	1.306	306619	1.407	92780	1.389
130970	1.552	97920	1.371	306619	1.416	112695	1.448
151200	1.578	117200	1.401	367726	1.380	129417	1.554
173990	1.592	134850	1.433	407785	1.430	146949	1.603
191900	1.506	134850	1.429			162622	1.624
211640	1.639	155700	1.409			180676	1.667
211640	1.544	174770	1.453			195123	1.680
231690	1.700	194160	1.497			205526	1.714
252500	1.578	209080	1.485			205526	1.738
271720	1.674					229617	1.761
292120	1.479					248947	1.747
312170	1.515					268999	1.776

312170	1.518			288429	1.793
332970	1.600			304231	1.825
360530	1.676			304231	1.850
392380	1.538			322571	1.845
				350076	1.828
				375004	1.841
				392653	1.857

Comparison of the measured deflection values of the reinforced concrete specimens and the values calculated using the fatigue damage function

Four specimens have already been tested. Specimen No. 1 in September 2009, No. 2 in November 2009, No. 3 in September 2013 and No. 4 in November 2013. Properties of the specimens are listed in Table 4. A comparison between the calculated and measured values is shown in Fig. 9 – Fig. 12.

The displacement was not measured continuously to prevent the fatigue damage of the inductive displacement transducer, thus each measurement had to be reinstrumented. This may result in the measurement errors as can be seen in Fig. 9. Still the trend is clearly observable.

Tab. 4: Properties of the tested specimens

Specimen no.	Age	f_{ck}	E_{init}
	[days]	[MPa]	[GPa]
#1	32	33.1	30.0
#2	61	34.2	34.3
#3	28	29.1	29.7
#4	60	34.0	30.0

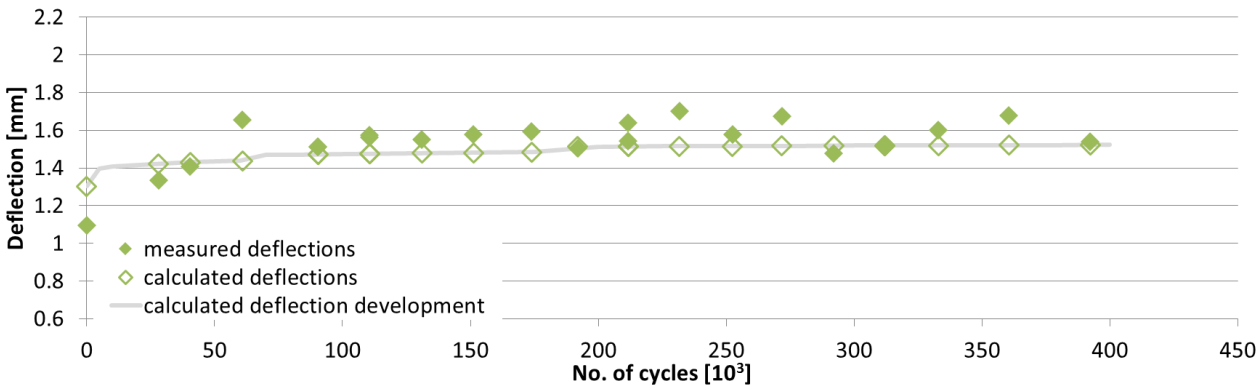

Fig. 9: Comparison of measured and calculated deflections for set #1

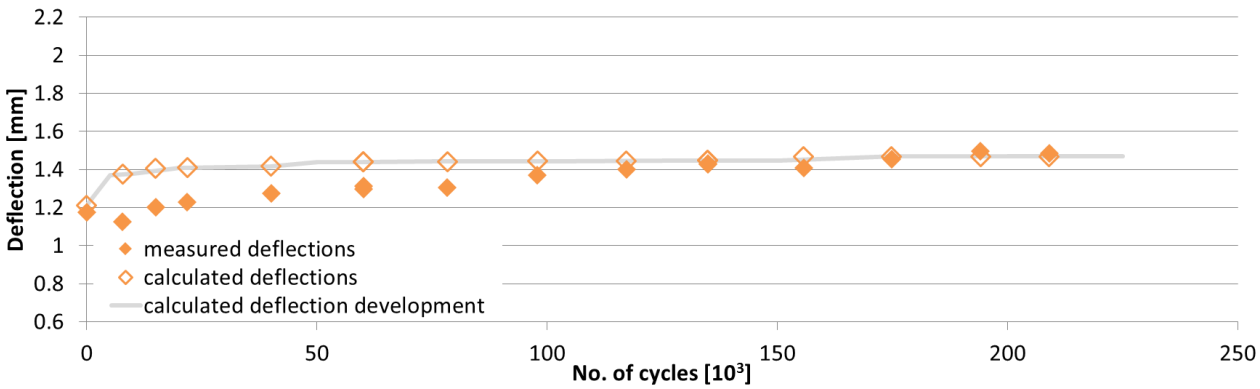

Fig. 10: Comparison of measured and calculated deflections for set #2

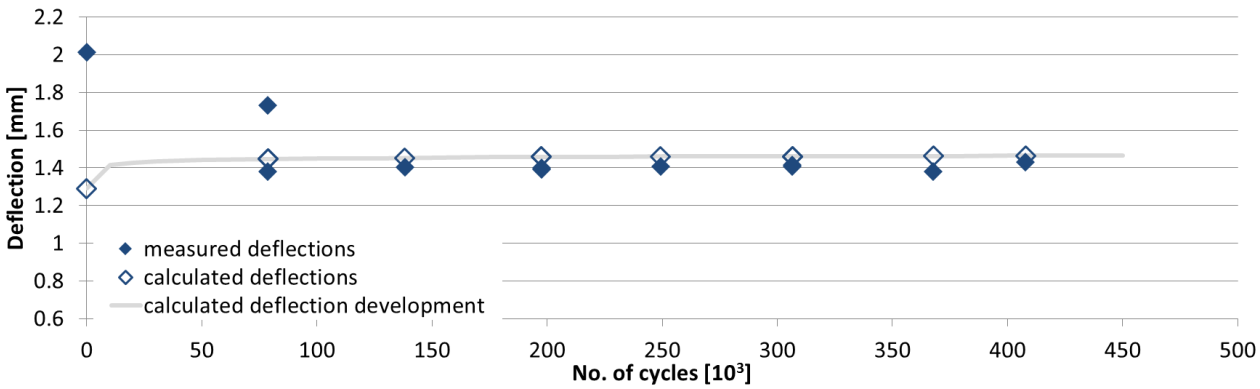

Fig. 11: Comparison of measured and calculated deflections for set #3

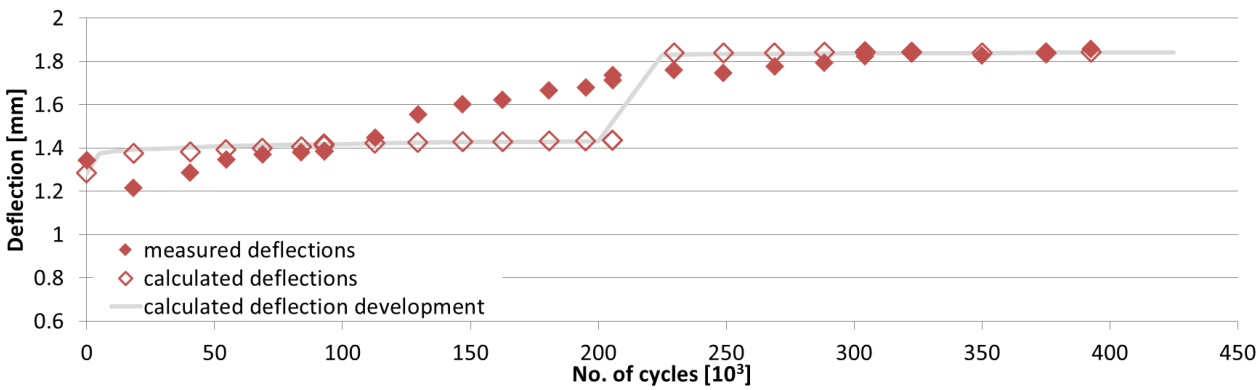

Fig. 12: Comparison of measured and calculated deflections for set #4

In Fig. 11 the decreasing slope at the beginning of cyclic loading and the difference in the second data point is probably a result of error in the first two measurements.

During the fatigue testing of the fourth specimen, a crack appeared in the direction of the principal tensile stress close to the support. This crack influenced the deflection measurements, as can be seen in Fig. 12. The crack opening developed between 110 thousand cycles and 230 thousand cycles. The increase in the deflection is about 0.4 mm. This increase was included in the comparison with the fatigue damage function.

Conclusions from the experimental verification of the fatigue damage function on the reinforced concrete specimens

The behaviour of the specimens corresponds with the trend calculated by the fatigue damage function, especially after first 100 thousand cycles. Within the first 100 thousand cycles, the values calculated with the fatigue damage function are higher than the measured values. It can be assumed, that this phenomenon is caused by the method of deflection calculation which uses moment of inertia of fully cracked cross section, when the cracks in specimens are not fully opened yet as described in [18] and Model Code 2010 [13].

The motivation for the approach presented here is to reflect the realistic distribution of the stress using the partial integration over the height. With this method, dividing the compressive zone into 20 layers provided optimal settings for the fatigue testing arrangement, and there was good agreement with the measured data. This approach should remove the conservativeness of the standardized model of fatigue assessment based on the analysis of the most stressed fibres.

Prestressed concrete specimen

The authors were allowed to incorporate their measurement system into the setup for the experiments described in [19].

The specimen was prestressed from one side by eleven 15.7mm prestressing tendons. The additional reinforcement was grade B500A. The strength class of the concrete of the prestressed slabs was prescribed as C 45/55. For the exact dimensions of the prestressed slab, see Fig. 13.

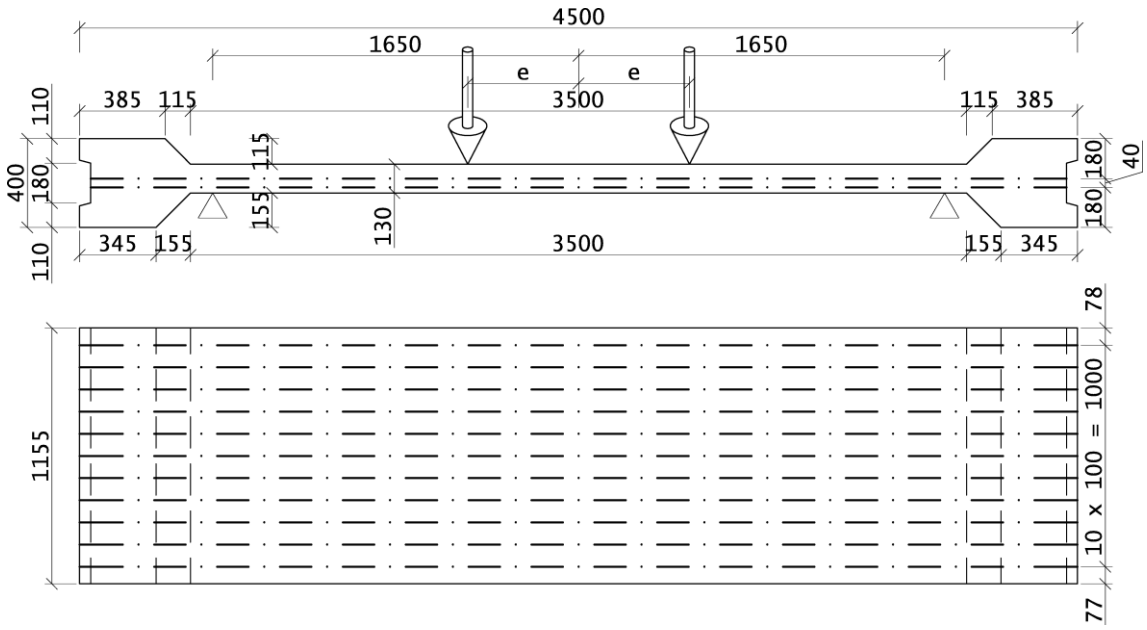

Fig. 13: Static scheme with the dimensions and the prestressing scheme in the slabs

For the evaluation of the deflections using the fatigue damage function, partial integration over the height of the specimen was used, as described above. However, the part of the cross-section subjected to tension was included. Values of the maximum of applied cycles *N* for the part in tension were evaluated according to Model Code 2010 [13] (eq. (7)), and are listed in Table 5 (positive values for compressive stress).

Tab. 5: Calculated values of the maximum applied cycles in tension according to Model Code 2010

Distance from the bottom fibres [m]	σ_{DL} [MPa]	σ_{DL+LL} [MPa]	N_k [-]
0.021	16.966	-0.331	1321789
0.018	17.441	-1.138	6.80E+09
0.015	17.915	-1.945	1.98E+08
0.011	18.390	-2.751	5744556
0.008	18.864	-3.558	167009
0.005	19.339	-4.365	4855
0.002	19.814	-5.171	141

The height of the prestressed specimen was divided into 40 layers to obtain similar precision as for the reinforced concrete specimens (each layer is ~3 mm in thickness). This division was based on a sensitivity analysis of the calculated deflection. When using coarse division, 5-10 layers, the difference between the calculated deflections was up to 10%. With a higher division, 20-25 layers, the difference was up to 4%. When using smooth division, 95-100 layers, the calculated difference was smaller than 1%. With the selected precision of 40 layers, the difference of the calculated deflections was up to 2%.

The influence of the cracks on the development of the increase in deflections due to cyclic loading needs to be discussed. The prestressed specimen passes through three stress distribution stages during cyclic loading. In the first stage, all fibres of the cross-section are subjected to compressive stresses; in the second stage, there is decompression in the bottom fibres; and, finally, in the third stage, the cross-section is divided into two zones - concrete subjected to compression, and concrete subjected to tension. The time sequence of these stages based on the characteristics of cyclic loading (sinusoidal loading) is illustrated in Fig. 14.

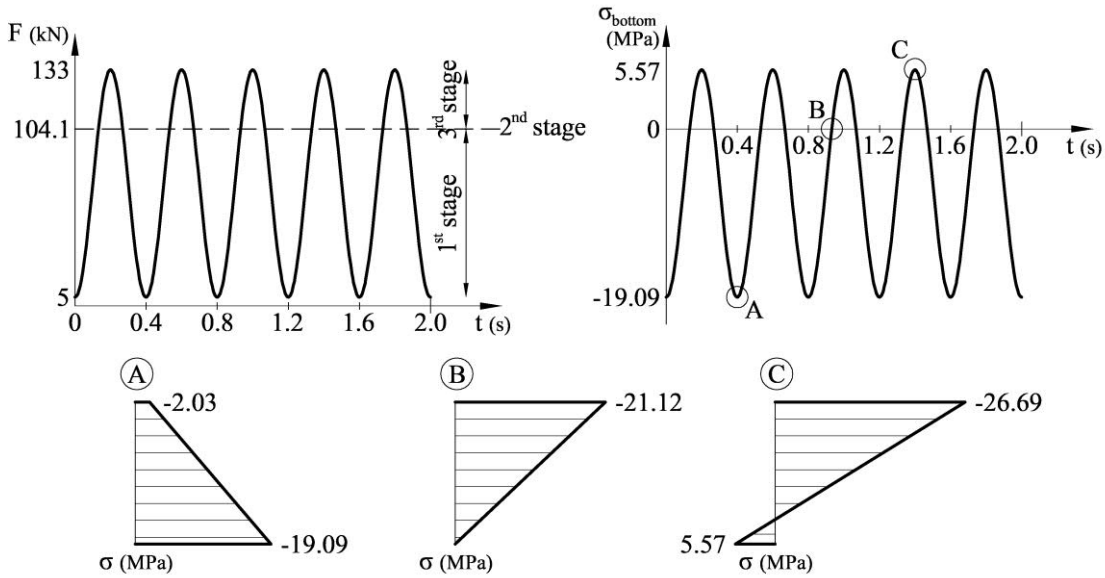

Fig. 14: Loading and stress development with emphasized stages

The major part of the stress distribution during cyclic loading corresponds to the first stage. In the third stage, the cracks open and the compressive zone gets smaller with the increase in the applied force. This means that, in the third stage, a stress reversal appears in the bottom fibres. In the approach presented here, the influence of the stress-reversal is taken into consideration.

In the approach followed by Eurocode 2 [15] (eq. (9)), the tensile stress is neglected and the minimum compressive stress is assumed to be 0 (for tensile stresses in the checked fibres). However, when assessing the fatigue endurance of a concrete specimen, the authors assumed that the difference in the stress distribution due to the opening of cracks has a low influence on the development of the fatigue damage function, or on the increase in deflections due to fatigue.

$$\frac{\sigma_{c,\max}}{f_{cd,fat}} \leq 0.5 + 0.45\frac{\sigma_{c,\min}}{f_{cd,fat}} \tag{9}$$

The evaluation of the decreased modulus of elasticity for each layer was based on the stress distribution for an uncracked cross-section with stress ranges corresponding to all three stages. Thus the bottom fibres are exposed to stress reversal.

The influence of the cracked cross-section on deflections was included by increase in the calculated values. The increment was calculated as the difference between the calculated deflections of the uncracked specimen and the cracked specimen at the time of cracking (n = 1 350 000 cycles). For both calculated deflections the deteriorative effect of the 1 350 000 applied cycles was taken into account.

To verify these assumptions, two approaches were compared. In the first approach, an evaluation was made of the fatigue damage function for the cracked cross-section (with the influence of a crack opening, thus without the stress-reversal in the bottom fibres after n = 1 350 000 cycles); in the second approach, an evaluation was made of the fatigue damage function for the uncracked cross-section (without the influence of a crack opening, thus with stress-reversal in the bottom fibres for all evaluated cycles). The results obtained with the first approach were extremely conservative (when compared with the measured data). The results obtained with the second approach showed good agreement with the measured data. The assumptions were verified for the testing arrangement of the experiment (described below).

Test layout

The specimen was subjected to four-point bending with a span length of 3300 mm. The arrangement is shown in Fig. 15.

Deflection measurements and loading history

During the experimental program, a total of five deflection measurements were made by an inductive track recorder. The measurements were conducted as dynamic deflection measurements, i.e. during the fatigue testing. The loading history of the test specimens was not continuous. This was due to the limitations of the laboratories.

Static analysis of prestressed slab specimens

An independent static analysis of the specimen was made in order to evaluate the maximum stresses S_{max} from the dead load and from cyclic loading.

The specimens were designed from concrete strength class C45/55, but the mean measured compressive strength value was 80 MPa. The modulus of elasticity was corresponding to Eurocode 2 for C80/95 (E_{cm} = 42 GPa). The measured static deflection was +6 mm.

The detailed FEM time-dependent analysis showed that the deformation of the specimen should be +5.8 mm in the middle of the span when loaded only by permanent loads, which corresponded to the deflections mentioned above.

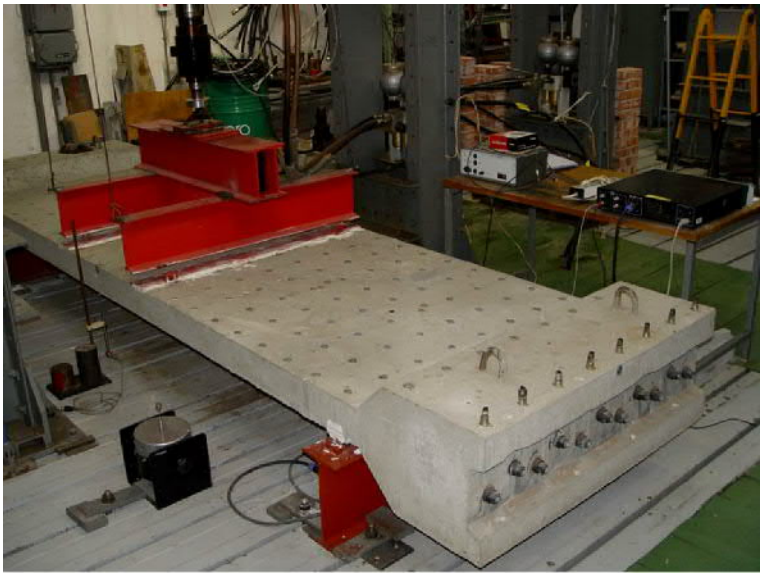

Fig. 15: Schematic layout of the experiments

Fatigue analysis of the pretressed specimens

Detailed fatigue analysis of the prestressed specimen was performed to predict the fatigue behaviour of the slab.

Considerations for the prestressed specimen were the same as in the case of the reinforced concrete specimens except that the fatigue endurance was calculated for the entire height of the specimen.

Table 6 shows the stress range for the load case applied to the prestressed specimen, together with the fatigue endurance in both characteristic and design values.

Tab. 6: Stress range due to dead load, dead load + cyclic load and fatigue endurance in design values with γ_M = 1.5 and γ_M = 1.0 according to Model Code 2010

Stress	Dead load	DL+LL	N γ_M = 1.5	N γ_M = 1.0
$\sigma_{top,fibers}$	-1.07	-26.69	7	4.49E+06
$\sigma_{bottom,fibers}$	-20.05	5.57		

Similarly as for the reinforced concrete specimens, the characteristic material properties values are used for verifying the fatigue endurance.

The verification of the fatigue endurance of the prestressed specimen according to Eurocode 2 [15] and Model Code 2010 [13] shows that the slab could not have experienced a compressive fatigue failure in the top fibres during the 2 268 570 load cases that it resisted.

Comparison of measured and calculated deflection values

A total of five deflection measurements were made. The time of the measurements, the measured deflections and the number of load cycles that were measured are shown in Table 7.

Tab. 7: Deflection measurements on Slab No. 2

Measurement No.	**Time** [days]	**Days between measurements** [days]	**No. of load cycles at measurement** [-]	**Measured deflections** [mm]
1	89	-	1 280 040	14.437
2	104	15	1 504 000	17.937
3	160	56	1 740 360	18.303
4	187	27	2 019 370	17.688
5	217	30	2 268 570	17.991

Fig. 16 shows the loading history of a prestressed specimen with the locations of the measurements marked.

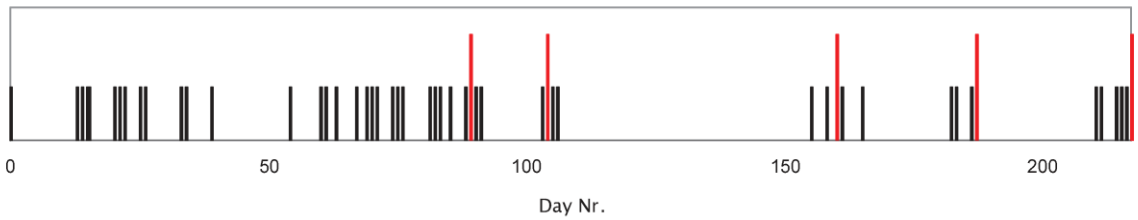

Fig. 16: Loading history of the prestressed slab with time of the deflection measurements marked

As was mentioned above, cracks propagated on the soffit of the slab after approximately 1 350 000 load cycles. These cracks resulted in an irreversible increase in the deformations between measurements 1 and 2 (see **Chyba! Nenalezen zdroj odkazů.**able 7).

Measured deflection values and values calculated using the fatigue damage function are summarized in Fig. 17.

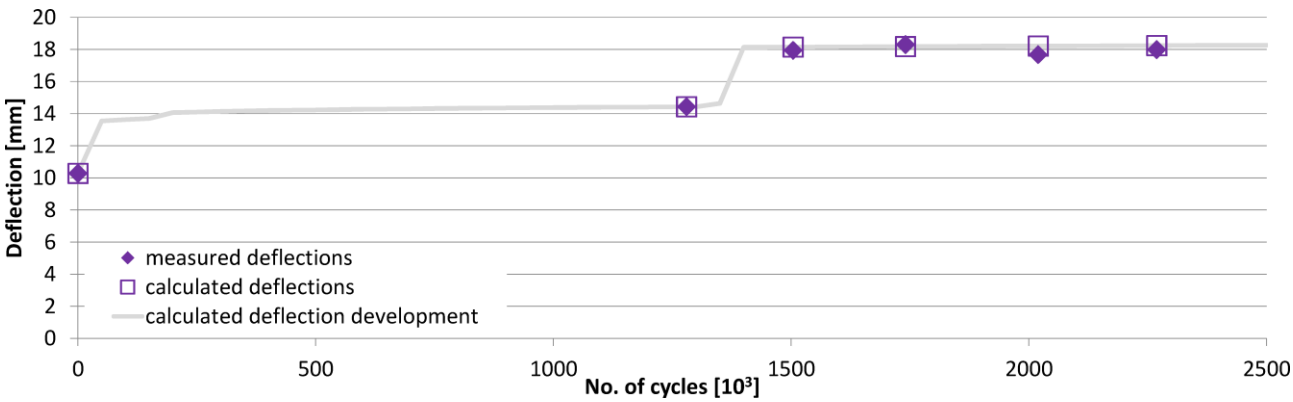

Fig. 17: Comparison of measured and calculated deflections of a prestressed specimen

With precision of 40 layers, the difference between the measured and calculated deflections is 5%. As was stated in section 3.3, the choice of this number of layers means that the difference in the calculated values is around 2%. The maximal potential error between the calculated and measured values is therefore assumed to be up to 7%.

The crack development in the bottom fibers of the prestressed specimen increased the uncertainty of the calculation. Within the rest periods, which were quite long (see Fig. 16), self-healing processes take place in the concrete:

- the stress concentrations on the tips of the cracks decrease due to relaxation of stresses,
- according to stress distribution within the prestressed specimen, the cracks close and can be healed by pore water reacting with unbonded cement.

A positive effect of rest periods on fatigue performance was observed in many cases, see e.g. [20].

The difference between static deflections and deflections caused by cyclic loading is emphasized in Table 8. There is a significant increase of 40% for the uncracked cross section, and 78% after crack development.

Tab. 8: Difference between static deflections and deflections within cyclic loading

Measurement No.	**Static deflection** [mm]	**Measured deflections** [mm]	**Calculated deflections** [mm]	**Measured / calculated deflections** [mm]	**Measured / static deflections** [mm]
1	10.286	14.437	14.430	1.001	140.36%
2	13.327	17.937	18.151	0.988	134.59%
3	13.327	18.303	18.184	1.007	137.34%
4	13.327	17.688	18.217	0.971	132.72%
5	13.327	17.991	18.244	0.986	134.99%

The predicted deflection behaviour of the prestressed specimen under cyclic loading shows that the initial values of the static deflection can increase up to 1.4 times without damage leading to the failure of an element. The prestressed specimen was not exposed to cyclic loading up to failure, so an even greater increase can be assumed before the slab collapses (i.e. enters the third phase of strain development under cyclic loading).

Conclusions from experimental verification of the fatigue damage function on prestressed slab specimens

Despite the limitations of the experiments, which were designed for a different purpose, the comparison between the measured deflection values of the prestressed specimen and the values calculated using the fatigue damage function shows very good agreement.

The deflections were measured from assumed n/N = 0.27 to n/N = 0.49, i.e. in the middle of the fatigue endurance of the specimen - the second phase of strain development under cyclic loading.

The principle presented here for evaluating the deflection, taking into consideration the cross-section in tension and neglecting the deteriorative influence of the infrequent stress distribution on a cracked cross-section, has proved to be a possible approach.

According to the experimental results, partial integration is a possible tool for evaluating the increased deflections due to cyclic loading for the prestressed specimens.

CONCLUSIONS

This paper has presented the fatigue damage function, a mathematical function for describing the strain development in concrete under cyclic loading, together with an experimental verification. The fatigue damage function produces a decreasing multiplier of the original modulus of elasticity at the start of cyclic loading, which represents the deteriorative effect of cyclic loading on a concrete structural element. With the help of the fatigue damage function, the increase in the deformations of cyclically loaded structural elements can be assessed and the total fatigue endurance and/or the remaining fatigue endurance can be predicted. This tool can be useful for example for the evaluation of the remaining useful fatigue life of bridges on which a load test was performed at the start of the operation.

The paper has presented an experimental verification of the fatigue damage function on reinforced concrete specimens and on a prestressed concrete slab. For calculating the increase in the deformations, a newly-developed method of partial integration over specimen height has been used to capture the real behaviour and the stress distribution of concrete specimens. This method can represent an improvement of the standard approaches, which appear to be very conservative. The method of partial integration has proved itself to be a useful tool for the evaluating the increase in deformations due to fatigue.

The measured deflection values and the values calculated using the fatigue damage function show very good agreement. A detailed analysis, and also the experimental measurements, have shown that the deflections of a cyclically loaded concrete structural element can reach as much as 140% (for reinforced concrete and also for prestressed concrete) of the initial static deflection without significantly reducing the load-bearing capacity and/or without any danger of the element failing due to fatigue failure of the concrete. Based on the performance of the specimens at the end of the testing, it can be assumed that an even higher increase in deflection is possible before the element fails.

ACKNOWLEDGEMENTS

Financial support from Czech Science Foundation grant project 13-30441S is gratefully acknowledged.

REFERENCES

[1] Mehmel A. Untersuchungen über den Einfluß häufig wiederholter Druckbeanspruchungen auf Druckelastizität und Druckfestigkeit von Beton. Technische Hochschule in Karlsruhe, Karlsruhe 1926.

[2] Graf O, Brenner E. Versuche zur Ermittlung der Wiederstandsfähigkeit von Beton gegen oftmals wiederholte Druckbelastung. Verlag von Wilhelm Erst & Sohn 1934.

[3] Sinha B, Gerstle K, Tulin L. Stress-strain relations for concrete under cyclic loading. ACI Journal Proceedings 1964;61:195-210.

[4] Holmen J. Fatigue of concrete by constant and variable amplitude loading. Bulletin No. 79-1, Division of Concrete Structures, NTH-Trondheim, Trondheim 1979.

[5] Tepfers R. Tensile Fatigue Strength of Plain Concrete. ACI Journal Proceedings 1979;76:919-933.

[6] Bahn B, Hsu C. Stress-strain behaviour of concrete under cyclic loading. ACI Materials Journal 1998;95:178-193.

[7] Ruiz G, Medeiros A, Zhang XX. Influence of loading frequency on the compressive fatigue behaviour of plain and fiber-reinforced concretes. In: Gomes JFS, Vaz MAP, editors. Proceedings of the 15th International Conference on Experimental Mechanics. Porto: Edições INEGI;2012.

[8] Hwan O. Fatigue analysis of plain concrete in flexure. Journal of Structural Engineering, New York 1986;112:273-288.

[9] Su E, Hsu T. Biaxial Compression Fatigue and Discontinuity of Concrete. ACI Materials Journal 1988;85:178-188.

[10] Hsu T. Fatigue of Plain Concrete. ACI Journal Proceedings 1981;78:292-305.

[11] Petryna Y, Krätzig W. Computational framework for long-term reliability analysis of RC structures. Computer Methods in Applied Mechanics and Engineering 2005;194:1619-1639.

[12] Horii H, Shin H, Pallewatta T. Mechanism of fatigue crack growth in concrete. Cement and Concrete Research 1992;14:83-89.

[13] CEN, EN 1992-1-1. Eurocode 2: Design of concrete structures - Part 1-1: General rules and rules for buildings. Brussels: European Committee for Standardization;2004.

[14] FIB, fib Bulletin 55: Model Code 2010 – Volume 1. Lausanne: International Federation for Structural Concrete;2010.

[15] CEB-FIP, CEB-FIP Bulletin No. 213/214 – Model Code 90. Lausanne: Comité Euro-International du Béton;1991.

[16] Foglar M. The strain development in concrete under cyclic loading. In: Bridge Maintenance, Safety, Management and Life-Cycle Optimization. Boca Raton: CRC Press; 2010, p. 3191-3195.

[17] Foglar M. Fatigue performance of pre-stressed and reinforced concrete. In: Advances and Trends in Structural Engineering, Mechanics and Computation. Cape Town: University of Cape Town; 2010, p. 371-374.

[18] Balász L, Bisch P, Borosnyói A. Design for SLS according to fib Model Code 2010. Structural Concrete 2013;14:99-123.

[19] Plachý T, Polák M. Vliv cyklického únavového namáhání na změnu modálních charakteristik prvku z předpjatého betonu. Acta Mechanica Slovaca 2006;10:395-400. (In Czech)

[20] König G, Danielewicz I. Ermüdungsfestigkeit von Stahlbeton- und Spannbetonbauteilen mit Erläuterung zu den Nachweisen gemäß CEB-FIP Model Code 1990 DAfStb.